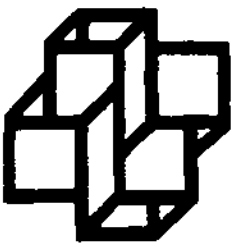

Laboratório Nacional de Computação Cientifica

LNCC – Nº 041/90

BIFURCATION OF THE SPIN-WAVE EQUATIONS

Ana Cascon
Jair Koiller[1]
Sergio M. Rezende[2]

ISSN 0101 6113

LABORATÓRIO NACIONAL DE COMPUTAÇÃO CIENTÍFICA - LNCC

RELATÓRIOS DE PESQUISA E DESENVOLVIMENTO

NOVEMBRO 1990

BIFURCATION OF THE SPIN-WAVE EQUATIONS

Ana Cascon
Jair Koiller[1]
Sergio M. Rezende[2]

[1] LNCC/CNPq and Instituto de Matemática, UFRJ, Cx. Postal 68530, 21945, Rio de Janeiro, Brasil.
[2] Departamento de Física, Universidade Fed. de Pernambuco, 50739, Recife, Brasil.

RESUMO

Estudamos as bifurcações da equação das ondas de spin que descrevem o bombeamento paralelo de modos coletivos em meios magnéticos. São propostos mecanismos para descrever os seguintes fenômenos dinâmicos: (i) excitação consecutiva de modos por bifurcações de autovalor nulo; (ii) bifurcações de Hopf seguidas (ou não) por cascatas de Feingenbaum de duplicação de períodos; (iii) fenômenos homoclinos locais e globais. Dois novos centros de organização para "rotas ao caos" são identificados; na classificação dada por Guckenheimer e Holmes [GH], uma delas é uma bifurcação *local* em codimensão dois com um par de autovalores imaginários e um autovalor nulo, para a qual muitas consequências dinâmicas são conhecidas; a outra é uma bifurcação homoclina *global* associado à quebra transversal de separatrizes, no limite em que o sistema pode ser considerado um Hamiltoniano sujeito à dissipação e bombeamento fracos. Indicamos o trabalho numérico e algébrico necessário para o estudo detalhado seguinto este programa.

ABSTRACT

We study the bifurcations of the spin-wave equations that describe the parametric pumping of collective modes in magnetic media. Mechanisms describing the following dynamical phenomena are proposed: (i) sequential excitation of modes via zero-eigenvalue bifurcations; (ii) Hopf bifurcations followed (or not) by Feingenbaum cascades of period doublings; (iii) local and global homoclinic phenomena. Two new organizing centers for routes to chaos are identified; in the classification given by Guckenheimer and Holmes [GH], one is a codimension-two *local* bifurcation, with one pair of imaginary eigenvalues and a zero eigenvalue, to which many dynamical consequences are known; secondly, *global* homoclinic bifurcations associated to splitting of separatrices, in the limit where the system can be considered a Hamiltonian subjected to weak dissipation and forcing. We outline what further numerical and algebraic work is necessary for the detailed study following this program.

Bifurcations of the Spin-Wave equations

Ana Cascon*, Jair Koiller** and Sergio M.Rezende***

Abstract: We study the bifurcations of the "spin-wave" equations that describe the parametric pumping of collective modes in magnetic media. Mechanisms describing the following dynamical phenomena are proposed: (i) sequential excitation of modes via zero-eigenvalue bifurcations; (ii) Hopf bifurcations followed (or not) by Feingenbaum cascades of period doublings; (iii) local and global homoclinic phenomena. Two new organizing centers for "routes to chaos" are identified; in the classification given by Guckenheimer and Holmes [GH], one is a codimension-two *local* bifurcation, with one pair of imaginary eigenvalues and a zero eigenvalue, to which many dynamical consequences are known; secondly, *global* homoclinic bifurcations associated to splitting of separatrices, in the limit where the system can be considered a Hamiltonian subjected to weak dissipation and forcing. We outline what further numerical and algebraic work is necessary for the detailed study following this program.

key words: spin-waves, bifurcations, chaotic dynamics, homoclinic behavior.

PACS numbers: 75.30.Ds , 76.50.+g

AMS/MOS: 58F14, 58F13, 34C35, 34C20

*Laboratório Nacional de Computação Científica, Rua Lauro Muller 455, Urca, 22290, Rio de Janeiro, RJ, Brazil,

**Laboratório Nacional de Computação Científica, Rua Lauro Muller 455, Urca, 22290, Rio de Janeiro, RJ, Brazil, and Instituto de Matemática da UFRJ, Caixa Postal 68530, 21945, Rio de Janeiro, Brazil.

*** Departamento de Fisica, Universidade Federal de Pernambuco, Cidade Universitária, 50739, Recife, PE, Brazil.

CONTENTS

1. Introduction.
2. Physical background:
   I. Basic facts about spin-wave instabilities.
   II. Equations of motion for parallel pumping and subsidiary resonance.
3. General aspects of the spin wave equations and overview.
4. Excitation of one mode. Phase portraits.
5. Excitation of a second (weak) mode: a transcritical bifurcation.
6. Hopf bifurcation.
7. Direct excitation of two modes; new transcritical bifurcations.
8. Heteroclinic phenomena at the origin: cycles.
9. A codimension -2 bifurcation: one zero, two imaginary eigenvalues
10. The near Hamiltonian limit for two modes: homoclinic phenomena.
11. Further topics for research.
12. Discussion.

Appendix 1. Stability of the equilibrium when $A^2+B^2 < C^2$.
Appendix 2. A center manifold calculation (by Prof.Richard H. Rand).
Appendix 3. A scheme to predict the Hopf-bifurcation parameter value.
Appendix 4. A Melnikov formula.

References.

Figure captions.

1. Introduction.

For over three decades it has been known that in a magnetic material subjected to a microwave frequency magnetic field, spin-wave instabilities can be excited as the field exceeds some threshhold value. Since the early days of spin-wave pumping experiments, it was observed that as the microwave power increases beyond this threshold, the radiation absorbed by the sample develops low-frequency coherent oscillations [HPW]. More complicated behavior, such as intermitency and period doubling routes to chaos, have been observed recently on physical experiments [AR,BJN]. Recently it has become clear that the origin of all these phenomena resides in the dynamic nonlinear interaction between few spin-wave modes. However, the spin-wave ODEs, given by equations first introduced by Zakharov et. al. [ZLS], have not so far been treated, in detail, by the mathematical theory of Dynamical Systems (for background on this theory, see e.g. Guckenheimer and Holmes [GH]).

The few-mode model has recently gained *formal* support from two different approaches. Gill and Zachary [GZ] have shown that the Landau-Lifshitz PDE, with damping and pumping terms added, has a maximal attracting set with finite-dimensional Hausdorff and fractal dimensions. This is in accordance with the fact that the dimensionality measured in physical experiments is low [YMNW,YM,AAR]. Dimensions of attractors calculated numerically in simulations of spin-wave equations with 2-modes were reported in [RA]. These two approaches will not be explored here. We just mention that the reduction of nonlinear PDEs to ODEs with few modes is becoming a common procedure [Ro]. Several authors have shown that computer numerical calculations with few spin-wave modes lead to results in good *qualitative* agreement with the experiments [RA, RA1, NOK, ON, BJN1,BJN2,CRP,GJ,JB,WBY].

For most physical systems it is not possible to describe the nonlinearities with theoretical models based on microscopic system parameters [GL]. A nice feature of spin-wave instabilities, which give them a special interest, is that they can be modelled by nonlinear equations derived from *microscopic* Hamiltonians with *well known* parameters. This provides a sound theoretical framework to interpret the experimentally observed signals. However, since a large number of spin-wave modes are in principle involved in the dynamics, it has not been possible, so far, to establish a *direct* quantitative comparison between theory and experiment.

It is to be expected that a detailed experimental study of the onset of auto-oscillations can provide a starting point for such direct comparison

[RAA,MW], as the Hopf bifurcation is amenable to mathematical analysis (numerical and analytical). Zhang and Suhl [SZ,ZS1] have shown that the infinite dimensional manifold of nearly degenerate spin-wave modes reorganizes itself into new, collective modes. Their work is based on simplified spin-wave equations, involving many approximations, which however become tractable by the method of center manifolds and normal forms [GH,C,RHA].

The main purpose of this paper is to point out that at least two other mathematical mechanisms, not previously reported, are present in the spin-wave equations. Potentially they can be "organizing centers" of observable physical behavior. We call attention to *homoclinic phenomena* associated to the Hamiltonian limit and to a codimension-2 bifurcation. According to the classification given by Guckenheimer and Homes [GH], the homoclinic behavior is "global" in the former and "local" in the latter situation. Near the Hamiltonian limit, all dissipation parameters are assumed to be small. In the codimension-2 bifurcation, just one of the dissipation parameters is supposed to be small. In this case, at a certain pumping power, one has an equilibrium with two conjugate purely imaginary and a zero eigenvalue, whose unfolding produces a wealth of dynamic phenomena.

2. Physical background.

i. Basic facts about spin-wave instabilities.

Spin waves are the collective elementary excitations of strongly-interacting spin systems [K,W], such as a ferromagnet. A spin wave with wave vector **k** has the spins precesssing with frequency ω_k about the equilibrium direction with phase planes perpendicular to **k**. The spin-wave dispersion relation $\omega_k(k)$ depends on the interactions between the spins and on the sample shape. Considering that the important spin interactions arise from the Zeeman (interaction with the external field H_o), exchange, crystalline anisotropy and dipolar energies, the dispersion relation, for $k << a^{-1}$ (a is the lattice parameter ≈ 10^{-7} cm) can be written as [K,W]

$$(2.1)\quad \omega_k = \gamma\,(H_z + H'_A + Dk^2)^{1/2}\,(H_z + H''_A + Dk^2 + 4\pi M \sin^2\theta_k)^{1/2}$$

where $H_z = H_o - 4\pi M N_z$, N_z is the demagnetization factor in the (z) direction of the external dc field H_o, $\gamma = g\mu_B/\hbar$ is the gyromagnetic ratio, M is the saturation magnetization, θ_k is the angle between **k** and H_o, D is the exchange stiffness, and H'_A and H''_A are effective fields arising from the anisotropy interaction. The shape of the dispersion relation is shown in Fig. 2.1. At field values H_o typical of laboratory electromagnets the frequency ω_k falls in the microwave range 1-10 GHz.

Spin waves are quantized, the quantum of which is a magnon with energy $\hbar\omega_k$ and momentum $\hbar$ **k**. At a finite temperature (T) magnons with energy $\hbar\omega_k$ are thermally excited with population n_k given by the Bose-Einstein distribution, which is typically of the order of 10^3 for k≈0. However, the population of magnons with selected **k** and ω_k can be driven to very large levels (≈10^{17}) by means of various microwave pumping instability processes.

In the parallel pumping process a microwave magnetic field h at a frequency ω_p is applied parallel to the static field H_o [M,SGM]. Because of the ellipticity in the spin precession (due to the dipolar interaction), the oscillating field couples to spin waves with frequency $\omega_k \approx \omega_p/2$. As a result, a uniform radiation (k=0) photon can drive parametrically *two* magnons with opposite wavevectors **k** and -**k**, thus conserving energy and momentum as illustrated in Fig. 2.1a. When the driving field h is larger than a certain threshold value h_c, the rate at which energy is pumped into the spin wave system exceeds that lost to the lattice through various

relaxation mechanisms. This causes the n_k magnon population to increase exponentially, until it reaches saturation caused by the nonlinear interactions.

In the perpendicular pumping configuration, the microwave field couples linearly to the uniform mode (k=0) and one observes a ferromagnetic resonance (FMR) absorption at $H_o = \omega_p/\gamma$. Although spin waves with $k \neq 0$ do not couple directly to the radiation they can be excited via magnon-magnon interactions. One can distinguish two main processes [S,WS]. In the first-order Suhl process, spin waves with $\omega_k = \omega_p/2$ in a $\mathbf{k},-\mathbf{k}$ pair can be driven parametrically by the uniform mode by means of the three-magnon interaction as shown in Fig. 2.1b. In this case the uniform mode is driven far off-resonance with $\omega_o = \omega_p/2$, so when the pumping exceeds a certain threshold one observes a *"subsidiary resonance"* at a field H_o roughly half the value for the main resonance. In the second order Suhl process a spin-wave pair k,-k is driven by two uniform mode magnons with frequency $\omega_o = \omega_p = \omega_k$ pumped by the microwave radiation via the four-magnon interaction.

In this paper we shall restrict the analysis to the parallel pumping and the subsidiary resonance processes . We will show that, somewhat surprisingly, they are described mathematically by identical equations .

The experimental arrangement to study spin-wave instabilities and nonlinear phenomena is quite simple. Microwave power from an oscillator is directed to a resonator via a precision attenuator and a circulator or a hybrid tee to allow observation of the reflected radiation. The resonator contains the sample and is located in a uniform dc field H_o whose value determines the wave-vector of the mode $\omega_k = \omega_p/2$ with minimum threshold. If the microwave power is below the threshold value ($h<h_c$) the reflection from the resonator is very small. As the power increases there is a sudden jump in the reflection, when $h \approx h_c$, as a result of the change in the sample susceptibility due to spin wave excitation. Further increase in the power usually leads to low-frequency (10kHz-1 MHz) amplitude modulations in the microwave reflection, the so called *auto-oscillation* , above a second threshold h_c'. The auto-oscillation can be observed directly with a diode detector connected to an oscilloscope or studied with a spectrum analyser. Further increase in power yields different types of complicated behavior, which have been observed in a variety of materials and situations.

II. Equations of motion for parallel pumping and subsidiary resonance.

The dynamics of spin wave systems can be studied by means of several different formalisms. We use here the method of second quantization, based on creation and annihilation magnon operators, $c_k\dagger$ and c_k, obtained from the spin operators with the Holstein-Primakoff transformations [WS,K,W]. The expectation value of the magnon operator $\langle c_k\dagger \rangle$ is proportional to the transverse value of the precessing magnetization $M^+ = M_x + i\, M_y$ and thus represents a spin-wave amplitude. Using a quantum mechanical formalism or a semi-classical approach one can show that the Hamiltonian for a spin-wave system pumped by a microwave field can be written as [WS,K,W]

(2.2) $$H = H^{(2)} + H^{(3)} + H^{(4)} + \ldots + H'(t)$$

where

(2.3) $$H^{(2)} = \Sigma_k \hbar\, \omega_k\, c_k\dagger\, c_k$$

is the Hamiltonian for a system of independent harmonic oscillators (magnons) with frequency ω_k. Summation ranges over positive and negative values of k. Terms $H^{(3)}$ and $H^{(4)}$ represent three and four-magnon interactions and $H'(t)$ describes the interaction with the microwave field.

The essential ingredient for the nonlinear dynamics is the coupling between two pairs of parametric magnons. This is provided by the four-magnon interaction [ZLS]

(2.4) $$H^{(4)} = \hbar\, \Sigma_{k,k'} (1/2\ S_{kk'}\, c_k\dagger c_{-k}\dagger\, c_k c_{-k'} + T_{kk'}\, c_k\dagger c_{k'}\dagger\, c_k\, c_{k'}) .$$

In simple ferromagnets this interaction arises [K] from the dipolar, anisotropy and exchange energies, but the latter is negligible for the small k-values excited in the microwave experiments. The interaction (2.4) couples the equations of motion for different k-modes giving rise to nonlinear behavior. The three-magnon interaction $H^{(3)}$ is not important for the nonlinear dynamics because it does not conserve energy for the two pair-modes. However, it is essential to provide the coupling of the microwave field to a spin-wave mode [S,WS].

In the case of parallel pumping we consider a uniform microwave field $h\cos(\omega_p t)$ applied in the (z) direction of H_o . In this case, for an isotropic infinite medium the driving term of the Hamiltonian becomes [K]

(2.5) $$H'_{||}(t) = 1/2\, h \sum_k \hbar\, \rho_k \exp(-i\,\omega_p t)\, c_k\dagger\, c_{-k}\dagger + h.c.$$

where $\rho_k = \gamma\, \omega_M \sin^2\theta_k \exp(-i2\varphi_k)/4\omega_k$ represents the coupling of the driving field with the $k, -k$ magnon pair, $\omega_M = \gamma\, 4\pi M$ and φ_k is the azymuthal angle of k. Notice that the coupling is strongest for spin waves propagating perpendicularly to H_o $(\theta_k=\pi/2)$.

In the case of perpendicular pumping the microwave field $h\cos(\omega_p t)$ couples directly only to the $k=0$ mode, and the driving term in the Hamiltonian (2.2) can be written as [K]

(2.6) $$H_\perp(t) = \hbar\, \gamma\, (SN/2)^{1/2}\, h\, (c_o\dagger \exp(-i\omega_p t) + h.c.)$$

where N is the number of spins S in the sample. In the first-order Suhl process, or subsidiary resonance, the $k=0$ mode drives a $k,-k$ magnon pair via the three-magnon interaction

(2.7) $$H^{(3)} = \hbar/2 \sum_{k\neq 0} F_k\, c_o\, c_k\dagger c_{-k}\dagger + h.c.$$

arising from the dipolar interaction. The interaction coefficient is given approximately by [WS]

(2.8) $$F_k = (2SN)^{1/2}\, \omega_M \sin 2\theta_k \exp(-i\,\varphi_k)$$

and is largest for spin waves propagating at an angle $\theta_k = \pi/4$. Since it is driven far off-resonance, the uniform mode behaves essentially like a virtual mode intermediary between the driving field and the spin wave pairs. Its amplitude acts like a classical variable [BJN] which can be obtained from the Heisenberg equation with (2.3) and (2.6),

(2.9) $$c_o = \gamma\, (SN/2)^{1/2}\, h \exp(-i\omega_p t) / [(\omega_p - \omega_o) - i\,\gamma_o]$$

With this approximation, interaction (2.6) becomes *identical* to the parallel pumping driving Hamiltonian (2.5) with the coupling coefficient given by (where $\omega_p = 2\omega_o = 2\omega_k$, $\omega_o - \omega >> \gamma_o$)

(2.10) $$\rho_k = \gamma\, \omega_M \sin 2\theta_k \exp(-i\varphi_k) / 4\omega_k \ .$$

This results shows, as we asserted previously:

Proposition 2.1 ([RA]). The first-order Suhl instability is described by the *same* equations as in the parallel-pumping process. In parallel pumping the modes with strongest coupling to the drive have $\theta_k = \pi/2$, whereas in the subsidiary resonance they have $\theta_k = \pi/4$.

Remark. It is worth recalling a statement found in the conclusion section of the seminal paper [ZLS]: "well away from resonance the phenomena which occur during transverse excitation are essentialy similar to those found for parallel excitation".

Using the Hamiltonian $H = H^{(2)} + H^{(4)} + H'(t)$ given by Eqs. (2.3-2.5) one obtains the equation of motion for the magnon operator c_k by means of the Heisenberg equation $dc_k/dt = [c_k,H]/i\hbar$. Since spin-wave modes are excited in pairs forming standing waves, one can assume $c_{-k} = \exp(iq_k)\, c_k$, where q_k is a real phase [BJN] . Taking the expectation value of the magnon operator and introducing the slowly varying amplitude

$$c_k = \langle c_k \rangle \exp(iq_k) \exp [\, i\, (\omega_p\, t)/2\,] \tag{2.11}$$

one obtains the equations of motion, which we call the *C-equations* :

Proposition 2.2 ([BJN]). Let $\Delta\omega_k = \omega_k - \omega_p/2$ be the detuning of mode k. Then

$$dc_k/dt = -(\gamma_k + i\,\Delta\omega_k)\, c_k - i\, h\, p_k\, c_k^* - i \sum_{k'} (S_{kk'}\, c_{k'}^2\, c_k^* + 2\, T_{kk'}\, |c_{k'}|^2\, c_k) \tag{2.12}$$

Note that the sample only supports modes that satisfy the boundary conditions, so that ω_k is discrete and $\Delta\omega_k$ is usually nonzero. The nonlinearly coupled equations (2.12) describe the dynamics of the interacting parametric (pair) modes. These equations have been used by Jeffries and coworkers [BJN] in numerical studies of perpendicular pumping.

For most part of this paper, instead of using (2.12), we shall prefer to work with the *Cooper - pair variables* σ_k [ZLS],

(2.13) $\sigma_k = c_k c_{-k} = n_k \exp(i\psi_k)$

where n_k is the number of magnons in the spin wave and ψ_k represents a phase. These variables have a simple physical interpretation [Wa]. If one strobes the precessing spins with a frequency $\omega_p/2$, n_k is proportional to the deviation in the z-component of the spin $\Delta S_z = S - S_z$ and ψ_k is the phase of the transverse spin component. Multiplying both sides of (2.12) by $c_{-k} = c_k$ (this follows from $\gamma_k = \gamma_{-k}$, $\Delta\omega_k = \Delta\omega_{-k}$ and $\rho_k = \rho_{-k}$) and adding the paired-equation we obtain the equations of the "S-theory" of Zhakarov, L'vov and Starobinets :

Proposition 2.3 ([ZLS]) (*S equations*) :

(2.14) $(1/2)\, \sigma_k/dt = -(\gamma_k + i\,\Delta\omega_k)\,\sigma_k - ih\,\rho_k\, n_k$

$$- i \Sigma_{k'} \,(S_{kk'}\, \sigma_{k'}\, n_k + 2T_{kk'}\, n_{k'}\, \sigma_k)$$

Using (2.13) and (2.14) one obtains the S-equations in polar form:

(2.15)

$$(1/2)\, dn_k/dt = -\gamma_k\, n_k + n_k \Sigma_{k'}\, S_{kk'}\, n_{k'}\, \sin(\psi_{k'}-\psi_k) - h\,\rho_k\, n_k \sin\psi_k$$

$$(1/2)\, d\psi_k/dt = -\Delta\omega_k - \Sigma_{k'}\, S_{kk'}\, n_{k'}\, \cos(\psi_{k'}-\psi_k) - \Sigma_{k'}\, 2T_{kk'}\, n_{k'} - h\rho_k \cos\psi_k$$

Note that $S_{ij} = S_{ji}$ and $T_{ij} = T_{ji}$ due to the symmetry of the physical interactions. Nevertheless, from the mathematician point of view, one can consider (2.14-15) as a more general set of equations, where these parameters can be taken asymmetric.

In this paper we will maily restrict the analysis to two modes. Since in yittrium garnet the nonlinear parameters S and T are of order 10^{-12} sec^{-1} and $\gamma_k \approx 10^6$ sec^{-1}, for numerical experiments [RA] equations (2.14) were divided by γ_1. Introducing normalized variables and parameters $'t' = \gamma_1 t$, $'n' = F n$, $'\sigma' = F \sigma$, $'T' = F^{-1}T$ and $'S' = F^{-1}S$, where $F = S/\gamma \approx 10^{-18}$, then $'n'$, $'T'/\gamma$ and $'S'/\gamma$ are of order unity. Omitting for clarity the quotation marks in the normalized variables and parameters (e.g., $'\Delta\omega_1' = \Delta\omega_1/\gamma_1$, etc.), equations (2.14) can be rewritten as [RA1]

$$(1/2)d\sigma_1/dt = -[1+i\Delta_1+i2(S_1+2T_1)n_1+4T_{12}\, n_2]\sigma_1 - i2S_{12}\,\sigma_2 n_1 - i\,R\,n_1$$

(2.16)

$$(1/2)d\sigma_2/dt = -[g+i\Delta_2+i2(S_2+2T_2)n_2+4T_{12}\, n_1]\sigma_2 - i2S_{12}\,\sigma_1 n_2 - i\,\alpha\,R n_2$$

where 'R' = $h\,\rho_1/\gamma_1$ is the control parameter, $g = \gamma_2/\gamma_1$, $\alpha = \rho_2/\rho_1$ and where for short we write $\Delta_k = \Delta\omega_k$.

Caveat: the appearance of extra factors of two in (S_1+2T_1) and T_{12}, S_{12} is due to the fact that we have a double contribution of the Cooper pairs. Parameter α represents the coupling strength between mode k_2 and the driving field, relative to that of mode k_1.

In the next section we discuss the basic aspects of the S-equations. In section 4 we will assume that only one mode is excited, not necessarily that one with minimum threshold.

3. General aspects of the spin-wave equations and overview.

In order to perform numerical experiments with a large number of modes, it is convenient to work with the cartesian version of the spin-wave equations (2.14) in a vectorialized form, which also shows that we have a *hierarchy* of equations as the number N of modes is increased. No harm is done by dropping the 1/2 factors in the left hand sides, which amounts to doubling the time scale: $t \leftarrow 2t$. Thus we get

$$\begin{pmatrix} x_k' \\ y_k' \end{pmatrix} = -\gamma_k \begin{pmatrix} x_k \\ y_k \end{pmatrix} + (\Delta_k + \Sigma_{k'} n_{k'} 2T_{kk'}) \begin{pmatrix} y_k \\ -x_k \end{pmatrix} + n_k \Sigma_{k'} S_{kk'} \begin{pmatrix} y_{k'} \\ -x_{k'} \end{pmatrix} - n_k \begin{pmatrix} 0 \\ R_k \end{pmatrix} \tag{3.1}$$

(I) (II) (III) (IV)

Here k and k' are taken both positive and negative, $R_k = h\,\rho_k$ and $\Delta_k = \Delta\omega_k$ for short.

This vectorialized form can also be helpful to understand the relative influence of its terms. (I) are the dissipative and (IV) the pumping terms. Terms (II) may be called "gyroscopic", since are tangent to the circles nj=const. The passage to polar coordinates form below shows that the terms (III) couple the relative phases.

At first sight, the presence of the factors $n_k = (x_k^2 + y_k^2)^{1/2}$ in the S-equations implies that one cannot linearize at the origin. This difficulty can be avoided using the C-equations (2.12), which are indeed more convenient to study the behavior at the origin (see section 7). Notice, nonetheless, that by *formally* adding N more equations

$$dn_k/dt = -\gamma_k n_k - R_k y_k + \Sigma_{k'} S_{kk'} (y_{k'} x_k - x_{k'} y_k) \tag{3.2}$$

(3.1) becomes a system of 3N ODEs in the variables (x_k, y_k, n_k) with *quadratic* nonlinearities (the C-equations are only 2N but have *cubic nonlinearities*). The augmented phase space possesses a 2N dimensional invariant manifold. One finds without difficulty that the linearization of the augmented system at the origin has eigenvalues $-\gamma_k$ (spurious) and

$$-\gamma_k \pm (R_k^2 - \Delta_k^2)^{1/2} \tag{3.3}$$

which, as expected, are the same as obtained directly from the C-equations. These are the relevant eigenvalues for the projected system. Thus one gets:

Proposition 3.1. The j-th mode unstabilizes at its *Suhl threshhold*

$$R^k_{Suhl} = (\Delta_k^2 + \gamma_k^2)^{1/2} \quad . \tag{3.4}$$

We point out that it is not necessarily true that the origin is a *global* attractor before the lowest threshold. Indeed, if the system has initial conditions far from the origin (physically this may happen due to "thermal excitation"), already for the 1-mode mode system it is possible to exist a competing attractor (see section 4). We antecipate from section 8 that chaotic behavior may occur immediately after the smallest threshold ! This phenomenon was called "hysteretic onset of chaos" in [BJN2].

The singularity at the origin of the S-equations can also be lifted by considering the spin-wave equations in its polar form (Takens' "blow-up", [GH, §7.2]).

$$\begin{aligned} dn_k/dt &= n_k \, [- \gamma_k - R_k \sin(\psi_k) + \Sigma_{k'} \, n_{k'} \, S_{kk'} \sin(\psi_{k'}-\psi_k) \,] \\ d\psi_k/dt &= -(\Delta_k + \Sigma_{k'} \, n_{k'} \, 2T_{kk'}) - R_k \cos\psi_k - [\, \Sigma_{k'} \, n_{k'} \, S_{kk'} \cos(\psi_{k'}-\psi_k) \,] \, . \end{aligned} \tag{3.5}$$

Using this formulation we will identify the mechanisms for sequential excitation of modes, Hopf bifurcations (section 6), a codimension 2 organizing-center (section 9), and homoclinic phenomena in the Hamiltonian limit (section 10). A simple calculation from (3.5) yields

Proposition 3.2. The divergence of the spin-wave system in the polar form is *constant* and *negative* ,

$$div = - \Sigma_k \gamma_k \tag{3.6}$$

so that, for the measure $dn_1 \ldots dn_N \, d\psi_1 \ldots d\psi_N = dx_1 dy_1 \ldots dx_N \, dy_N / (n_1 \ldots n_N)$, volumes are shrunk at that constant rate. In particular, no sources or totally unstable periodic orbits can exist.

As we have seen in section 2, the physical considerations yielding the quantal Hamiltonian impose that for the spin-wave systems (3.5) the

coefficients S_{ij} and T_{ij} must be symmetric. Dropping the dissipation terms in (3.5), there is a Hamiltonian structure [A,AM]. An interesting feature is that the *pumping terms can be incorporated into the Hamiltonian* (this idea is also used in other physical systems; see section 12).

Proposition 3.3. The symplectic form is given by

(3.7) $\Omega = \sum dx_k \wedge dy_k / n_k = \sum dn_k \wedge d\psi_k$

and the Hamiltonian is ([ZLS, eqs. (3.9), (3.10)])

(3.8) $-H = \sum_{k,k'} [(1/2)\, S_{kk'}\,(x_k x_{k'}+y_k y_{k'}) + n_k n_{k'}\, T_{kk'}\,] + \sum_k (\Delta_k\, n_k + R_k\, x_k)$,

where $x_k x_{k'}+y_k y_{k'} = n_k n_{k'} \cos(\psi_k-\psi_{k'})$, $R_k = \rho_k\, h$.

In the case of equal damping or all modes, i.e., $\gamma_i = \gamma$ $(1\le i\le N)$ the equations can be written as $z = J\, \mathrm{grad}_z\, H(n,\psi) - \gamma\, (n,\psi)$, $J = \begin{matrix} 0 & 1 \\ -1 & 0 \end{matrix}$, $z=(n,\psi)$.

These *dissipative Hamiltonian systems* [Dr,VDG, OV], maintain some of the features of usual Hamiltonian systems. For instance, eigenvalues of the ODE at fixed points come in pairs, symmetric with respect to the line $\mathrm{Re}z = -\gamma/2$ (plus the conjugates when complex), and Krein's classification [A] of eigenvalue types applies. An implication is that, in many cases, Hopf bifurcations must be preceded by Krein collisions. Such features do not hold when the dissipation coefficients are different.

When there is no pumping ($h=0$) nor dissipation, the Hamiltonian is clearly invariant under the rotational symmetry $\psi_k \to \psi_k+\psi$, yielding the conserved momentum

(3.9) $I = \sum_k n_k$.

Equilibria of the reduced systems (with $h=0$) are called *relative equilibria* for the total system [A,AM]. They correspond to periodic orbits in which the n_j are constant and the phases evolve with the same rate, thus with constant phase differences. The search for these periodic solutions, and more interestingly, their perturbations as the pumping parameter h is turned on and the dissipation is considered, will be left for future work. We just observe that if only the dissipation is added,the relative equilibria in this case are destroyed. Setting $n_j'=0$ in (3.5) then $A(n_1,\dots,n_N) = (\gamma_1, \dots, \gamma_N)$, where A is an antisymmetric matrix: $a_{ij} = S_{ij} \sin(\psi_j-\psi_i)$. It is impossible to

find a solution with all $n_j \geq 0$ (with at least one >0), because then $0 = {}^t n A n = {}^t n.(\gamma_1, .., \gamma_N) > 0$, a contradiction. However, if one allows asymmetric S_{ij}, it is possible to construct families of relative equilibria for the spin wave equations with dissipation.

The two-mode system with $h=0$ and no dissipation is completely integrable in Liouville's sense. For small h, KAM theory applies, so the motion is trapped between invariant tori. The nonintegrable O(h) perturbation produces transversal homoclinic phenomena, associated to separatrix splitting. Transversality persists for small enough dissipation. For small values of h and γ_1 we provide in section 9 a quantitative description, using "Melnikov's method" [GH,Li,Wi,WiH].

4. Excitation of one mode. Phase portraits.

In this section we study the simplest possible situation, where just one of the modes, say n_k, is excited: $n_{k'}=0$, $k'\neq k,-k$ (mode -k is the Cooper pair). The phase space is the half-cylinder $n\geq 0$, $\psi \in [-\pi,\pi]$. The equations of motion are

$$\begin{aligned} dn_k/dt &= -\gamma_k n_k - n_k R_k \sin\psi_k \\ d\psi_k/dt &= -\Delta_k - S_k n_k - R_k \cos\psi_k . \end{aligned} \tag{4.1}$$

where for short we denote $S_k = 2S_{kk} + 4T_{kk}$. The factors of two come from collecting the Cooper-pair contributions ($S_{kk} = S_{-k,-k}$, $T_{kk} = T_{-k,-k}$).

For the remaining of this section we will drop the subscripts k. We rescale time, $t \leftarrow \gamma t$, so now $\gamma=1$. The equations depend on three parameters R,Δ,S (to undo, just replace R,Δ,S by $R/\gamma, \Delta/\gamma, S/\gamma$ in all formulas below).

The following heuristic argument shows that if $S\neq 0$, then all trajectories eventually enter a bounded region: if n is very large, the term Sn dominates in ψ', so one can average over the angle ψ in the equation for n'. The averaged equation is just -n. On the other hand, "escapes" are possible if S is set equal to zero. This can be shown explicitly, since for $S=0$ the analytical solution can be obtained by separation of variables:

$$dn/n = [(1 + R\sin\psi) /(\Delta+R\cos\psi)]d\psi \qquad (S=0). \tag{4.2}$$

We will assume $S\neq 0$. Proposition 4.1 describe the relevant facts about equilibrium points. Their stability character depend on the eigenvalues μ_1,μ_2 of the Jacobian

$$J = \begin{pmatrix} -1-R\sin\psi & -nR\cos\psi \\ -S & R\sin\psi \end{pmatrix} \tag{4.3}$$

calculated at the points where $dn/dt = 0$, $d\psi/dt = 0$.

Proposition 4.1. One mode system: Equilibrium points.

A) With $n=0$. Equilibrium points do not exist if $R<|\Delta|$. If $R\geq|\Delta|$: $\cos\psi=-\Delta/R$.

Let $p=(R^2-\Delta^2)^{1/2} \geq 0$.

A1. $\sin\psi = -(1-(\Delta/R)^2)^{1/2}$: $\mu_1+\mu_2 = -1$, $\mu_1.\mu_2 = p(1-p)$.
i) $p>1$: Saddle. ii) $0\leq p<1$: Node attractor.

A2. $\sin\psi = +(1-(\Delta/R)^2)^{1/2}$: $\mu_1+\mu_2 = -1$, $\mu_1.\mu_2 = -p(1+p)$. Saddle

B) With $n\neq 0$. Equilibrium points do not exist if $0\leq R<1$. If $R\geq 1$: $\sin\psi=-1/R$.

B1. $\cos\psi = (1-(1/R)^2)^{1/2}$. $n=(1/S)\{-\Delta-(R^2-1)^{1/2}\}$.
B2. $\cos\psi = -(1-(1/R)^2)^{1/2}$. $n=(1/S)\{-\Delta+(R^2-1)^{1/2}\}$.

In both cases, $\mu_1+\mu_2 = -1$, $\mu_1.\mu_2 = -SnR\cos\psi$
One has saddle point or attractor. See Fig.4.1.

The attractor with $n\neq 0$ is a *focus* for all points sufficiently far in the stable branch L^s (Fig.4.1). We will be particularly interested in Hopf bifurcations; however, this type of bifurcation can never occur if only one mode is present, because the real part of the eigenvalue is always - 1/2 , that is, negative (in general, - $\delta_1/2$). Nonetheless, through nonlinear interaction with a second, weakly excited mode, this focus on the L^s branch is the "seed" for a Hopf bifurcation, as we will show in section 6.

Proposition 4.2. (Nature of the attractor with $n\neq 0$.) Let $q=(R^2-1)^{1/2}$. The condition for a focus attractor is $q|\Delta+q|>1/4$ if $S<0$, and $q|\Delta-q|>1/4$ if $S>0$. This is the case for R sufficiently large in branch L^s .

It is instructive to sketch all possible different portraits in the two-dimensional phase plane. One will be surprised by the number of bifurcations already present in this elementary setting (where just one mode is present). Fig.4.2 depicts the phase portrait with $\Delta=1$, $S=-1$, $R=1.2$. There are here two *competing* attractors, one with $n=0$, and the other with $n\neq 0$. Eventually, for R greater than $(1+\Delta^2)^{1/2}$ (Suhl threshold) only one attractor survives, that with $n\neq 0$. Notice that hysteresis occurs: mode $n=0$ excites directly to a

finite value when the Suhl threshold is exceeded (jump bifurcation); when the control parameter is slowly decreased, the steady state follows the solid line in Fig.4.1.

Considering the augmented 3-dimensional system with the "dummy" equation R'=0 added, we note the elementary appearance of two dimensional (inside the three dimensional phase x R-space) *center manifolds* , born when a real eigenvalue changes sign. In fact, J has a zero eigenvalue (the other being equal to -1) at ($n=0$, $\cos\psi=-\Delta/R$) when (i) $R=|\Delta|$ or when (ii) $R^2=1+\Delta^2$, $\sin\psi=-1/R$. Case (i) corresponds to the coalescence of the saddle A2 and the node attractor A1 . Case (ii) corresponds to the coalescence of the equilibrium point B) in branch L with A1. Here A1 changes from attractor to saddle as R^2 exceeds $1+\Delta^2$, and this is consistent with B) being an attractor in Fig.4.1 , (a),(c) and a saddle in Fig.4.1, (b),(d). Here either the axis $n=0$ or the branch L (with a stable part L^s and an unstable L^u) contain the equilibria in the center manifold.

As we mentioned, in cases b) and d) of Fig.4.1 there is a stable nonzero steady state above $R=1$, prior to the Suhl threshold (ST). Suppose mode 1 has the smallest ST, and assume that it is greater than γ_2/ρ_2. Then it is a mathematical possibility that mode 2 attains a nonzero steady state before mode 1, provided the system is given suitable initial conditions. See section 8 for numerical examples. On the other hand, excitation begins at the smallest Suhl threshold when the microwave power is applied to samples in thermal equilibrium (all $n_k=0$).

5. Excitation of a second (weak) mode: a transcritical bifurcation.

Physically there are infinitely many spin-wave modes involved in the instability process. Suhl and Zhang [SZ,ZS] point out that, "as the signal increases beyond threshhold, an entire manifold of pairs enters the picture. In fact for parallel pumping as well as for the subsidiary resonance, this is already the case at threshhold". Using a simplified set of equations, those authors have used center manifold theory to explain that the dynamics is dominated by essentially two collective normal modes.

Hence we consider the S-system described by (3.5) with *two* modes. To avoid unecessary numerical factors present in (3.5) when the Cooper-pair contribution is added, we redefine its coefficients by $T_{12} \leftarrow 4T_{12}$ and $S_{12} \leftarrow 2S_{12}$, $S_k \leftarrow 2(S_{kk}+2T_{kk})$. So we have

$$
\begin{aligned}
dn_1/dt &= n_1\,[-\gamma_1 + n_2 S_{12}\sin(\psi_2-\psi_1) - R_1\sin(\psi_1)\,] \\
d\psi_1/dt &= -\Delta_1 - T_{12}\,n_2 - S_1\,n_1 - n_2 S_{12}\cos(\psi_2-\psi_1) - R_1\cos\psi_1 \\
dn_2/dt &= n_2\,[-\gamma_2 + n_1 S_{21}\sin(\psi_1-\psi_2) - R_2\sin(\psi_2)\,] \\
d\psi_2/dt &= -\Delta_2 - T_{21}\,n_1 - S_2\,n_2 - n_1 S_{21}\cos(\psi_2-\psi_1) - R_2\cos\psi_2\ .
\end{aligned}
\tag{5.1}
$$

We take the equilibrium points corresponding to L^s (Fig.4.1), maintaining $n_2=0$. This is the more relevant situation, but the analysis below can be replicated to the branch L^u, if one is interested in following the bifurcations of unstable equilibrium points as well. Thus

$$
\begin{aligned}
n_1^e &= (-\Delta_1/S_1) + (R_1^2-\gamma_1^2)^{1/2}/|S_1| \\
\sin\psi_1^e &= -\gamma_1/R_1
\end{aligned}
\tag{5.2}
$$

and the signs of $\cos\psi_1^e$ are given in Fig.4.1, depending on those of S_1. Although $n_2=0$, we nevertheless search for values ψ_2^e such that $\psi_2' = 0$. We must solve:

$$\Delta_2 + T_{21}\,n_1^e + R_2\cos\psi_2^e + n_1^e S_{21}\cos(\psi_1^e-\psi_2^e) = 0$$

Substituting (5.1) this equation becomes

Case $A^2+B^2 < C^2$. Since mode $n_2=0$, ψ_2 is just a "mathematical entitity" following the "nonphysical" T-periodic orbit (ψ_2' never vanishes)

(5.6) $$n_1 = n_1^e\ ,\ \psi_1 = \psi_1\ ,\ n_2 = 0\ ,\ \psi_2 = \psi_2(t)\ ,\quad 0\le t\le T\ .$$

where

$$d\psi_2/dt = -\Delta_2 - n_1^e\, S_{21}\, \cos(\psi_1^e - \psi_2) - T_{21}\, n_1^e - R_2\, \cos\psi_2$$

(5.7)

$$T = \int_0^{2\pi} d\psi_2 / \left[-\Delta_2 - n_1^e S_{21}\, \cos(\psi_1^e - \psi_2) - T_{21}\, n_1^e - R_2\, \cos\psi_2\right]$$

The following is a natural question: is it possible that the onset of the second mode has its origin on the Floquet unstabilization of this periodic orbit? We show in Appendix 1 that the answer is *negative* : the periodic orbit remains stable as long as $A^2+B^2 < C^2$. A residue calculation yields

(5.8) $$T = 2\pi/(C^2-(A^2+B^2))^{1/2}\ .$$

Thus the period becomes infinite at a parameter value h# where $E(h) = A^2+B^2 - C^2$ changes sign from negative to positive. At this value equations (5.4) have a double solution, corresponding to a degenerate equilibrium point (saddle-node bifurcation) for the restricted dynamics in ψ_2. Subsequently, this equilibrium point separates into two, of different stability types, as we now proceed to discuss.

Case $A^2+B^2 > C^2$. The two equilibrium points are

(5.9)
$$\cos\psi_2^e = [AC - B\ \mathrm{sqrt}(A^2 + B^2 - C^2)]/(A^2 + B^2)$$
$$\sin\psi_2^e = [BC + A\ \mathrm{sqrt}(A^2 + B^2 - C^2)]/(A^2 + B^2)\ .$$

(5.10)
$$\cos\psi_2^e = [AC + B\ \mathrm{sqrt}(A^2 + B^2 - C^2)]/(A^2 + B^2)$$
$$\sin\psi_2^e = [BC - A\ \mathrm{sqrt}(A^2 + B^2 - C^2)]/(A^2 + B^2)\ .$$

For the restricted 1-dimensional dynamics of ψ_2 (5.9) is a stable equilibrium, while (5.10) is unstable. Thus (5.10) has no interest and can be discarded. Proposition 5.1 below gives the behavior of $(n_1^e, n_2=0, \psi_1^e, \psi_2^e)$ with ψ_2^e given by (5.9). The Jacobian matrix has the following structure:

$$(5.11) \qquad J = \begin{pmatrix} 0 & J_{12} & J_{13} & 0 \\ -S_1 & -\gamma_1 & J_{23} & 0 \\ 0 & 0 & \lambda_3 & 0 \\ J_{41} & J_{42} & -S_2 & \lambda_4 \end{pmatrix}$$

where the nonzero coefficients are given in Table 1 below. The eigenvalues of J can be read off directly as $\lambda_1, \lambda_2, \lambda_3, \lambda_4$, where λ_1, λ_2 are the eigenvalues of the left-upper 2x2 block corresponding to the 1-mode system (4.3) at $(\bar{n}_1, \psi_1)$. Loosely speaking, λ_3, λ_4, determine the stability of n_2, ψ_2, respectively.

Table 1. Coefficients of the Jacobian matrix.

$$\lambda_3 = -\gamma_2 - R_2 \sin\psi_2^e + n_1^e S_{21} \sin(\psi_1^e - \psi_2^e)$$

$$\lambda_4 = -\gamma_2 - \lambda_3$$

$$J_{12} = -n_1^e (R_1^2 - \gamma_1^2)^{1/2}$$

$$J_{13} = S_{12} n_1^e \sin(\psi_2^e - \psi_1^e)$$

$$J_{23} = -T_{12} - S_{12} \cos(\psi_2^e - \psi_1^e)$$

$$J_{41} = -T_{21} - S_{21} \cos(\psi_2^e - \psi_1^e)$$

$$J_{42} = -S_{21} n_1^e \sin(\psi_2^e - \psi_1^e)$$

Remark 1 : only parameter S_2 is not present.

Remark 2 : Since $\lambda_3 = -\sigma_2 + Ay-Bx$, $Ax+By=C$ and $x^2+y^2=1$, elementary algebra yields the following useful formula:

(5.12) $\quad \lambda_3 = -\sigma_2 \pm (A^2+B^2-C^2)^{1/2}$.

The - branch corresponding to (5.10) has no interest for us since λ_3 is always negative, while λ_4 is always positive. In a sense the - branch is just an artifact of the polar coordinates: it would not appear if we work with the C-equations. For the + branch, corresponding to (5.9) we may have a zero eigenvalue bifurcation exciting mode n_2.

Proposition 5.1. For the equilibrium solutions (5.9), corresponding to the + branch of (5.12), λ_3 changes sign at values h^* such that $E(h^*)=\sigma_2^2$. Note that λ_4 is always negative.

The spectral analysis of (5.11) can be readily done. It suffices to do it at $h=h^*$ where $\lambda_3(h^*)=0$. Notice that $\lambda_4(h^*)= -\sigma_2 < 0$.

Proposition 5.2. At $h=h^*$ a suitable basis for center manifold calculations is given by the colums of P, ordered as $\{v_3,v_4,v_1,v_2\}$

$$P = \begin{matrix} a & 0 & 1 & 0 \\ b & 0 & 0 & 1 \\ 1 & 0 & 0 & 0 \\ c & 1 & d & e \end{matrix} \qquad P^{-1} = \begin{matrix} 0 & 0 & 1 & 0 \\ -d & -e & -c+ad+be & 1 \\ 1 & 0 & -a & 0 \\ 0 & 1 & -b & 0 \end{matrix}$$

$$P^{-1} J P = \begin{matrix} 0 & 0 & 0 & 0 \\ 0 & \lambda_4 & 0 & 0 \\ 0 & 0 & 0 & J_{12} \\ 0 & 0 & -S_1 & -\sigma_2 \end{matrix}$$

Table 2. Coefficients for eigendecomposition of J at $h=h^*$

$\lambda_4 = -\gamma_2$

$b = S_{12} \sin(\psi_2^e - \psi_1^e)/ (R_1^2-\gamma_1^2)$

$a = (-\gamma_1 b + J_{23})/S_1$

$c = (S_2-J_{41}a-J_{42}b)/\lambda_4$

$d = [J_{41}(\gamma_1+\lambda_4)-S_1J_{42}]/[\lambda_4(-\gamma_1-\lambda_4)-J_{12}S_1]$

$e = [\lambda_4 J_{42} + J_{41}J_{12}]/[\lambda_4(-\gamma_1-\lambda_4)-J_{12} S_1]$

Proposition 5.3. Suppose that at the point P where L^s starts (Fig.4.1) one has $\lambda_3 (P) < 0$. This is the case if $\gamma_2^2 > E(P) > 0$. The values of h^* at which $\lambda_3=0$ are roots of the biquadratic polynomial (top signs correspond to cases b)d) of Fig.4.1) :

$$p_1^2 h^4 + 2 (p_0 p_1 - 2 p_1^2 q_0^2) h^2 + p_0^2 + 4 \gamma_1^2 q_0^2 = 0 . \tag{5.14}$$

$$\begin{aligned} p_1 &= p_1^2 T_{21}^2/S_1^2 + [\, p_2 \pm S_{21} p_1 /|S_1|\,]^2 \\ p_0 &= \gamma_2^2 \pm 2 (\gamma_1^2 S_{21}/|S_1|) [p_2 /p_1 \pm S_{21} /|S_1|\,] \\ &\quad - \gamma_1^2 T_{21}^2/S_1^2 - S_{21}^2 (\Delta_1^2 + \gamma_1^2)/S_1^2 \\ &\quad + (\Delta_2 - T_{21} \Delta_1 / S_1)^2 \\ q_0 &= -[\,(S_{21}^2 \Delta_1/(S_1|S_1|\,) \pm \Delta_1 S_{21} p_2/(S_1 p_1)\,] \\ &\quad - \Delta_2 T_{21}/|S_1| + T_{21}^2 \Delta_1/(S_1|S_1|) \end{aligned} \tag{5.15}$$

As stressed before, care must be taken since we may have introduced spurious roots. Examples will be given in the next two sections. As one moves along branch L^s ($n_1^e \neq 0$, $n_2=0$) , varying the control parameter h, there may exist h^* at which λ_3 changes from negative to positive.

It is well known from the theory of dynamical systems that at this moment a one dimensional center manifold with $n_2 \neq 0$ is born [C,RHA] . In the cases of physical interest, we have

Proposition 5.4. In this center manifold, for $0 < h-h^* << 1$ there is a new stable equilibrium point with $n_1 = n_1^e(h^*) + 0(h-h^*)$ and $0 < n_2^e = 0(h-h^*)$, for $h > h^*$, arising from a transcritical bifurcation.

Appendix 2 gives the main features of a center manifold algebraic calculation, kindly emailed to us by Prof. Richard H.Rand.

6. Hopf bifurcation.

The onset of a steady state containing both a strong and a weak mode paves the way for further bifurcations. One one hand, one may consider the imbedded hierarchy of ODEs with more modes and investigate the appearance of equilibria with three or more nonzero modes. Each new mode arises at a zero-eigenvalue bifurcation; after the excitation of a finite number of modes, a Hopf bifurcation may eventually take place. On the other hand, we may at the outset restrict the study to the two-mode system.

Let's discuss the latter possibility. Consider parameter choices such that λ_1, λ_2 are complex conjugate with negative real parts $-\gamma_1/2$ for the 1 mode system (Proposition 4.2). Mode 2 is excited as soon as h surpasses h^*, and the behavior of λ_1, λ_2 changes. Numerical experiments indicate indeed that there is a domain of parameters such that the strong mode-weak mode steady state suffers a Hopf bifurcation at a higher value $h_{Hopf} > h^*$. Furthermore, there is a (possibly reduced) parameter range such that the resulting limit cycle will suffer a cascade of period doublings to chaos.

In the example of Fig.6.1 we describe numerically the onset of the auto-oscillations, using parameter values as in [RA1,Fig.8], namely (using equation (2.16)): $\alpha = 0.7$, $g = 5.0$, $\Delta_1 = \Delta_2 = 0$, $S_{11}+2T_{11} = -1$, $S_{22}+2T_{22} = 0.5$, $S_{12} = 2.5$ and $T_{12} = 1.125$. Caveat: changing the notations to those of (5.1), $\gamma_1 = 2$, $\gamma_2 = 10$, $S_1 = -4$, $S_2 = 2$, $S_{12} = 10$, $T_{12} = 9$. In the experiments, n_2 was excited at $h^* \approx 2.4$. This agrees very well with the theoretical prediction $h^* = 2.394566$, using (5.14) with the top signs.

Notice that in Fig.6.1 the strong-weak steady state for $2.4 < h < 3.1$ appears to be moving uniformly on a straight line. The onset of auto-oscillations occurs at $h\# \approx 3.1$. Fig. 6.2 depicts the behavior of the four eigenvalues. The pair of conjugate eigenvalues λ_1, λ_2 corresponding to the n_1 mode when $n_2 = 0$, initially moves on the line $Re\lambda = -1$. When $h^* \approx 2.4$ mode n_2 is excited to a non-zero steady state. At this value the pair λ_1, λ_2 *sharply* turns its direction, moving towards the imaginary axis. From Fig.6.2 we see that it is reasonable to approximate this motion by a straight line. Thus we used the change on the eigenvalues immediately after $h^* \approx 2.4$ to predict, by linear extrapolation, the value $h\# \approx 3.15$ for the crossing, which is in good agreement with the results. The absolute value of the eigenvalues when they cross the imaginary axis is ≈ 5.4. Correspondingly, the numerically observed frequency of auto-oscillations at $h = 3.2$ is about 5.46. Moreover, the amplitude of the oscillation $n_1(t)$ was observed to vary, as expected, like $(h-h\#)^{1/2}$.

For other numerical examples, see [RA1, Figs.3,4,5] . The Hopf bifurcation was observed on physical experiments [RAA]. See Fig.6.3, taken from [RACK] .

Proposition 6.1. The mathematical mechanism for the Hopf bifurcation of the strong-weak equilibrium consists on the deviation of λ_1, λ_2 (eigenvalues of the strong-mode) from the line Re $\lambda = -\gamma_1/2$, due to the coupling with the weak mode.

At the moment we do not have a formal proof, but we present a few remarks in support of Proposition 6.1. First, the behavior of the eigenvalues in Fig.6.2 resembles qualitatively to what one knows rigorously in the case of equal dissipations [DL]. The movement of the eigenvalue pair corresponding to the weak mode, in the direction of negative real values, is compensated by the movement of the Hopf-bifurcating pair in the other direction. Observe that practically linear motions of (n_1,n_2) and (λ_1, λ_2) are occurring even though $\gamma_1 = 2$ is not very small.

Following this linear scheme, in Appendix 3 we outline an approximate method to predict the control parameter value corresponding to a Hopf bifurcation, using computer algebra. We plan to pursue the details in future work. As far as we know, this type of study was pioneered by J.P.Keener [Ke,Ke1] which followed, using computer algebraic methods, the locus both on phase and parameter spaces, of Hopf bifurcations for a chemostat model and for a predator-prey system.

We point out that the first period doubling is generically associated to the dissolution of the 2-dimensional center manifold containing the Hopf limit cycle. The parameter value associated to this bifurcation can be predicted on the basis of Floquet theory, using semianalytical procedures. See [Rd, Kap, KM]. In this way it is possible to obtain, approximately, the region of parameters where the Feigenbaum route to chaos occurs.

In section 9 we sketch the unfolding of the degenerate situation when $\gamma_1 = 0$, where the Hopf bifurcation occurs together with the excitation of n_2 at h^*. In some related situations it is now known the existence and uniqueness of the limit cycle which arises in such unfolding [CSG].

We now briefly discuss the possibility of the onset of a third mode, etc. prior to the Hopf bifurcation. We take the spin-wave equations with three modes in the polar form, and we consider the strong-weak steady state with two nonzero modes, and a vanishing third mode $n_3 = 0$. Looking for a

(mathematical) value $\psi_3{}^e$ such that $d\psi_3/dt = 0$, one obtains a similar situation as (5.3-4) (but the algebraic implementation is harder). As before, mode n_3 unstabilizes at a zero eigenvalue bifurcation. If the corresponding control parameter value is less than the value for h_{Hopf} calculated for two modes, the third mode will be excited before that 2-mode-Hopf bifurcation having a chance.

In fact, since a great number of modes have nearby thresholds, it is likely that several modes will be excited to a steady steate *prior* to the Hopf bifurcation. This is our interpretation of the statement in Suhl and Zhang [SZ] that "the first Hopf bifurcation (which results in a limit cycle) sets up a collective mode of the entire manifold of spin waves".

7. Direct excitation of two modes; new transcritical bifurcations.

Nakamura and coworkers [NOK, ON] showed that in the case where all coefficients are symmetric, a family of equilibrium solutions $n_1=n_2=n$ emanates from the origin as soon as the Suhl threshold is surpassed. Let

(7.1) $\Delta_1=\Delta_2$, $\gamma_1=\gamma_2$, $\rho_1=\rho_2$, $S_1 = S_2$, $T_{12} = T_{21}$, $S_{12} = S_{21}$.

Without loss of generality we may assume $\gamma_1=1$, $\rho_1=1$. The equilibrium solutions $n_1=n_2=n$, given by

(7.2) $n = - [\Delta \pm (R^2-1)^{1/2}] / (S_{12} + S_1 + T_{12})$

may undergo jump bifurcations/hysteresis (analogously to Proposition 4.1).

The Jacobian matrix is

(7.3) $$J = \begin{matrix} 0 & r & 0 & u \\ S & -1 & T & 0 \\ 0 & u & 0 & r \\ T & 0 & S & -1 \end{matrix}$$

with

(7.4) $$u = n^2 s_{12} \quad , \quad T= -S_{12} - T_{12} \quad , \quad S = - S_1$$
$$r = - R n \cos\psi - n^2 S_{12}$$

The roots of the characteristic polynomial

(7.5) $p_{char} = x^2(1+x)^2 + (rS+uT)(1+x)+(S^2-T^2)(r^2-u^2)$.

were obtained by computer algebra:

(7.6) $-1/2 \pm (1/2)[1 +4(r\pm u)(S\pm T)]^{1/2}$

Note that this is in agreement with the symplectic relations for dissipative Hamiltonian systems with equal damping [Dr,OV]: the eigenvalues are pairwise symmetric with respect to the line Re λ = -1/2.

Proposition 7.1. Hopf bifurcation does not take place along the $n_1=n_2$ branch. Two of the eigenvalues are never zero, actually being real negative or complex conjugate with negative real parts. One of the other eigenvalues will be zero, producing transcritical bifurcations, when (r+u)(T+S) or (r-u)(S-T) vanish.

It is easy to find values of R such that r+u vanishes: either the Suhl threshold $R = (1 + \Delta^2)^{1/2}$ at which $n=0$ or

$$R = 1 \ , \quad R = [\, 1 \ + (\Delta/Q)^2]^{1/2} \qquad (Q = T + S) \tag{7.7}$$

For the case r-u=0 we obtained, using computer algebra, the biquadratic polynomial $aR^4 + bR^2 + c = 0$ with

$$\begin{aligned} a &= (-Q^2 - 4\, S_{12}^2 + 4\, Q\, S_{12}) \\ b &= \Delta^2\, (8\, S_{12}^2 - 4\, S_{12}\, Q + Q^2) + 2Q^2 - 8Q\, s_{12} + 8 s_{12}^2 \\ c &= \Delta^2\, (-8\, S_{12}^2 + 4\, S_{12} Q - Q^2) - 4\, S_{12}^2\, \Delta^4 - Q^2 - 4\, S_{12}^2 + 4\, Q\, S_{12} \end{aligned} \tag{7.8}$$

whose roots are the Suhl threshhold again and

$$R^2 = \frac{[\,4\, S_{12}^2(\Delta^2 + 1) + (Q^2 - 4\, Q\, S_{12})]}{Q^2 - 4\, Q\, S_{12} + 4\, S_{12}^2} \tag{7.9}$$

In general, the values of the roots are different so only one real eigenvalue vanishes at a time (codimension 1 bifurcations). There are some exceptions, though. At the Suhl threshhold r and u both vanish, so at the origin $n_1=n_2=0$ there is a double zero eigenvalue. Here a local unfolding analysis could be done using techniques such as in [GH, §7.3]. Special choices also lead to double real eigenvalues. For instance, if $\Delta=0$ or $Q=1$ then r-s and r+s vanish at the same time. This is also the case when the the following relation holds: $Q(1-4S_{12}^2) = 2\, S_{12} \pm 4\, S_{12}^2$.

In [ON, Fig.1] regions of parameter space were depicted corresponding to values of R at which the equilibrium solution with $n_1=n_2$, $\psi_1=\psi_2$ changes stability. The specific type of unstabilization was not reported, and it has been generally thought as Hopf bifurcation. However, we showed here that this is *not* the case. Namely, the unstabilization *always* corresponds to the

passage of a real eigenvalue through zero, producing transcritical bifurcations.

In Fig.7.1 we show the periodic orbits which lead, as h increases, to the strange attractor in [NOK]. In the notations of (2.16), $\gamma_i=1$, $\Delta_i= -1$, $S_{ii}+2T_{ii}=1$, $T_{12}= -0.75$, $S_{12}=-0.4$; following (5.1), $\gamma_i=2$, $\Delta=-2$, $S=4$, $T_{12}=-6$ and $S_{12}=-1.6$. The Suhl threshhold, here identical for the two modes, is $h_S = \sqrt{2}$. Mode $(n_1\neq 0, n_2=0)$ with $n_1= [1+\sqrt{R^2-1}]/2$ unstabilizes at $R^*= 3.1113$, obtained by (5.14) with the bottom signs. We followed numerically the periodic orbits from h=4.4 back to h=3.65, using as initial guess for each R a point in the orbit corresponding to the preceeding value of R. Below R=3.65 the solution seems to be attracted to a fixed point $n_2=0$, $n_1\neq 0$, even though R is still quite larger than R^*.

Remark. It is possible to work analytically under slightly more general assumptions. We consider systems with asymmetrical coefficients and look for *phase locked* solutions $\psi_1=\psi_2$ (with both $n_1\neq 0$, $n_2\neq 0$). Since at the equilibrium point we must then have

$$\sin\psi_1 = -\gamma_1/R_1 = \sin\psi_2 = -\gamma_2/R_2 \tag{7.10}$$

it follows that we need just to assume the equality $\gamma_1/\rho_1 = \gamma_2/\rho_2$. Under this assumption, the equilibrium pair (n_1,n_2) satisfies the linear system (the solution (7.2) is recovered in the case of symmetric coefficients) :

$$\begin{matrix} S_1 & T_{12}+S_{12} & n_1 & & -\Delta_1 - R_1\cos\psi_1 \\ & & & = & \\ T_{21}+S_{21} & S_2 & n_2 & & -\Delta_2 - R_2\cos\psi_2 \end{matrix} \tag{7.11}$$

Of course, only solutions with $n_1, n_2 > 0$ have physical interest. We have not been able yet to accomplish the algebraic calculation of eigenvalues in this more general case. Nonetheless, we can at least guarantee that, for small perturbation of the symmetrical case, there is no Hopf bifurcation. We also observe that for small enough values of the difference $\gamma_1/\rho_1 - \gamma_2/\rho_2$, these equilibrium solutions may be continued into fully general asymmetrical solutions (i.e., with slightly different phases $\psi_1\neq\psi_2$).

In the case of symmetrical coefficients, phase locked solutions were computed numerically for up to 100 modes by Lim and Huber [LH].

8. Heteroclinic phenomena at the origin: cycles.

To study the behavior of the spin-wave system at the origin, it is more convenient to consider the C-equations. Dropping the cubic interaction terms in (2.12), the complex modes c_k uncouple and one gets for any given mode the linearized equations $dc/dt = -(\gamma + i\Delta)c - i R c^*$ (subscripts ommitted). The origin is a spiral focus for $0 < R < |\Delta|$. At $R=|\Delta|$ the imaginary parts of the conjugate eigenvalues vanish; for $|\Delta| < R < \sqrt{(\Delta^2+\gamma^2)}$ one gets a node. At $R= \sqrt{(\Delta^2+\gamma^2)}$ one of the real negative eigenvalues vanishes (Suhl threshold) and the origin is a saddle for $R > \sqrt{(\Delta^2+\gamma^2)}$.

We denote the critical values by $h^k_{fn} = |\Delta_k|/\rho_k$ and $h^k_{ns} = \sqrt{(\Delta_k^2+\gamma_k^2)}/\rho_k$. Here fn means "focus to node" and ns "node to saddle".

The numerical experiments described below indicate that heteroclinic recurrence fenomena at the origin is present for certain parameter values. Since the recurrent behavior was found as soon as one of the modes becomes unstable, we may have here a situation of homoclinic bifurcations with nonhyperbolic equilibria [De], yielding "blue sky catastrophes" [AM,CDF].

In Fig.8.1-8.3 the same parameter values as in [BJN2, Figs.9,10] are used, namely, in the notations of eq. (2.12), $\gamma_1=\gamma_2=1$, $\rho_1=\rho_2=1$, $\Delta_1= -1.884$, $\Delta_2= 1.254$, $S_1+2T_1 = S_2+2T_2 = -0.286$, $S_{12} = 4.078$, $T_{12}=0$. For mode 1 we get $h^1_{fn}= 1.884$, $h^1_{ns} = 2.133$, while for mode 2, $h^2_{fn} = 1.254$, $h^2_{ns} = 1.604$. Thus mode 2 unstabilizes at 1.604, value for which the linearization of mode 1 is a *spiral* focus. This at first sight suggests Silnikov's homoclinic recurrence [GH, Si,Si1]. Indeed, we found a similar behavior in the numerical experiments. Unstabilization was first seen at h=1.64. Initially, the oscillations resembled an aperiodic intermittence, frequency beginning low but increasing fast, as shown in Fig.8.2. For h=1.685 we observe a "pseudo Silnikov" behavior for mode 1, as in Fig.8.3 (why "pseudo"?; see the remark below). For h >1.80 one gets periodic oscillations similar to Fig.9 of [BJN2].

In Fig.8.4-8.6 we use the following parameter values, with notations of (2.12): $\gamma_1= 1$, $\gamma_2=2$, $\rho_1=1$, $\rho_2=0.7$, $\Delta_1= 0.8$, $\Delta_2 = -0.5$, $S_1+2T_1 = -0.5$, $S_2+2T_2 = 0.5$, $S_{12} = 2.5$, $T_{12}=0.125$. For mode 1 we get $h^1_{fn}= 0.8$, $h^1_{ns} = 1.2806$, while for mode 2, $h^2_{fn} = 0.35$, $h^2_{ns} = 2.95$. Thus mode 1 unstabilizes at 1.28 where mode 2 is a *node* attractor. Homoclinic recurrence here could be analogous (but not exactly; see remark below) of a type discussed by Holmes [H]. In the numerical experiments we found that the origin in $n_1 x n_2$ space becomes unstable at h=1.27. For h=1.30 Fig.8.5 suggests that there may be a

heteroclinic cycle between the origin and (n_1=1.6, n_2=0). Fig.8.6 shows the dependence $f^2 = (h/h_c)^2 - 1$ between pumping and frequency. Extrapolation to h=0 yields h_c=1.274.

Remark . The chaotic behavior observed in Fig.8.3 was classified by Bryant, Jeffries and Nakamura [BJN2, §IIIC] as of "Silnikov's type". We wish to point out that although the numerical observations may be *similar* to those one sees in Silnikov's case, the dynamical explanation must be *different* . The designation of "relaxation vs. spiking behavior" actually introduced by those authors seems more appropriate.

Silnikov's phenomenon arises on systems which can be reduced to a 3-dimensional phase space; one assumes that an equilibrium point has two complex conjugate eigenvalues with negative real parts, and one real positive eigenvalue. The one dimensional unstable manifold emanating from the equilibrium is a homoclinic orbit, returning to the equilibrium as an spiralling orbit in the local stable manifold.

What seems to be happening here, on the other hand, is a bona fide *four* dimensional phenomenon, which, as far as we know, has not yet been studied in detail by the methods of Dynamical Systems. Consider a (c_1,c_2) phase space such that the c_1 and c_2 complex planes are invariant manifolds for the dynamics. Suppose that the origin is a global attractor, of spiral-focus type, for the restricted dynamics in the c_1-plane, and a saddle for the restricted dynamics in the c_2-plane. Since the unstable manifold for the full (c_1,c_2) system is contained in the c_2 plane, there is no chance that this unstable 1 dimensional manifold returns directly to the origin in Silnikov's fashion. Nevertheless, the unstable manifold *can* return to the origin, either directly as a homoclinic loop in the c_2 plane, or through a *cycle* connecting critical elements in full (c_1,c_2) phase space [PBMB]. One scenario is as follows: there is a orbit connecting the origin and a stable equilibrium $c_2^e \neq 0$ viewed in the restricted c_2-dynamics. However, suppose (c_1=0, c_2^e) is an unstable equilibrium viewed in the full dynamics; the unstable 1-dimensional manifold emanating from this point may also be contained in the *three* dimensional stable manifold of the origin. Actually this 1-dimensional unstable manifold may connect to other critical elements until a cycle to the origin is formed.

A detailed study of this situation is in order, both from the numerical and the theoretical viewpoint. One possible direction of research is to find an algebraic approximation for the dynamics, continuing the Hartman-Grobman linearizing scheme outside the invertible region [OCR, ROD].

On the experimental side, we remark that recent measurements produced results similar to the type of numerical solutions [RACK].

9. A codimension-2 bifurcation: one zero, two imaginary eigenvalues.

We go back to the S-equations in the form (5.1) and consider the Jacobian matrix (5.11) at $(n_1^e, \psi_1^e, n_2=0, \psi_2^e)$. If we set $\gamma_1 = 0$ then at the control parameter value h^* we get one *zero* eigenvalue $\lambda_3=0$ and two *imaginary*

(9.1) $\quad \lambda_{1,2} = \pm i\,\omega \quad , \quad \omega = (J_{12}\, S_1)^{1/2}$.

This is is a codimension-2 bifurcation, discussed in Guckenheimer and Holmes [GH,§7.4]. Two small parameters are needed to unfold it: here these parameters are precisely γ_1 and $h-h^*$. The assumption of very small γ_1 is physically reasonable, since spin-wave systems have large relaxation times.

The nature of the bifurcations taking place for one real zero, two purely imaginary eigenvalues is not yet completely understood ([GH,§7.4,7.5], [CSG]). Here we will just outline the computational-algebraic steps necessary to characterize this bifurcation, for the spin-wave system, in terms of the presently available mathematical theory.

Step 1 . Let P be the matrix of Proposition 5.2 with column vectors reordered as $(J_{12}\, S_1)^{1/2} v_1,\ v_2\ , v_3\ ,\ v_4$. Then

$$P^{-1}JP = \begin{pmatrix} 0 & -\omega & 0 & 0 \\ \omega & 0 & 0 & 0 \\ 0 & 0 & 0 & 0 \\ 0 & 0 & 0 & \lambda_4 \end{pmatrix} \tag{9.2}$$

We set $\mu = h - h^*$, and regard μ, γ_1 as new dynamical variables. We are in the standard form used for a center manifold calculation with additional dummy equations $\mu'=0$, $\gamma_1'=0$. Products of μ or γ_1 with themselves or with the other variables are considered as *quadratic* terms in the Taylor expansions. See [C,RHA] for background and computer codes.

Step 2 . Call x,y,z the center manifold coordinates (besides the two additional dummy coordinates μ,γ_1). The linear part is of the form

$$\begin{matrix} 0 & -\omega & 0 \\ \omega & 0 & 0 \\ 0 & 0 & 0 \end{matrix} \qquad (8.3)$$

and the quadratic and higher order terms contain the *five* coordinates. Transform to cylindrical polar coordinates (r,θ,z).

Step 3 . Find the truncated, θ-averaged-out, planar system in (r,z)-phase space. *The main computational problem is finding this k-determined jet* . Guckenheimer and Holmes consider in some detail the case of the 2-jet $dr/dt=\mu_1 r+arz$, $dz/dt=\mu_2+br^2-z^2$ [GH, eq. (7.4.9)] , but this seems not to be the correct guess here, since our system has fixed points at $z=0$ for all μ_1,μ_2 . A more plausible form is $dr/dt = \mu_1 r + arz$, $dz/dt = \mu_2 \pm r^2 - z^2$ [GH,eq.(7.4.42)] , which now has a transcritical bifurcation of the fixed point at $z=0$. Another possibility is the Z_2-symmetric pitchfork bifurcation [GH, eq.(7.5.10)].

Step 4 . Restore the sufficient higher order terms to the planar system, study the corresponding phase portraits. Finally, consider the implications for the full three-dimensional flow, when the θ-dependent terms are restored. Identify the distinct phase portraits and dynamical phenomena to regions of the *original* parameters.

Among the delicate dynamical phenomena known to exist [GH] for the "one real zero, two purely imaginary eigenvalues" bifurcation: (i) invariant tori with two frequencies, one fast and one slow; (ii) transverse homoclinic orbits with Silnikov behavior. It seems important to find numerically trajectories of these types for the spin-wave system.

10. The near Hamiltonian limit for 2 modes: homoclinic phenomena

Although the Hamiltonian structure was introduced in section 3 under the hypothesis of symmetric T_{ij} and S_{ij}, in the case of two modes we are able to allow $S_{12} \neq S_{21}$, $T_{12} \neq T_{21}$. Setting $\gamma_1 = \gamma_2 = h = 0$, we get the constant of motion

$$z = n_1/S_{12} + n_2/S_{21} \quad . \tag{10.1}$$

The following reduced system is obtained, where $\psi = \psi_1 - \psi_2$ is the phase difference, and $\Delta_{12} = \Delta_1 - \Delta_2$:

$$\begin{aligned} dn_1/dt &= -S_{21}(S_{12}\, z - n_1)\, n_1 \sin\psi \\ d\psi/dt &= -\Delta_{12} - S_{21}\,(S_{12}\, z - 2n_1)\cos\psi + (S_2 - T_{12})S_{21}\, z - \\ &\qquad - [(S_1 - T_{21}) + (S_2 - T_{12})S_{21}/S_{12}]\, n_1 \end{aligned} \tag{10.2}$$

This system is Hamiltonian, with conjugate variables $p = n_1$, $q = \psi$, and Hamiltonian function $H = pF$, where F is given by

$$\begin{aligned} F(p,q) = &-\Delta_{12} + (S_2 - T_{12})S_{21}\, z - (p/2)[(S_1 - T_{21}) + (S_2 - T_{12})S_{21}/S_{12}] + \\ &+ S_{21}\cos q\,(p - S_{12}\, z) \quad . \end{aligned} \tag{10.3}$$

Depending on the choice of parameters, there are several different types of phase portraits for H, with a rich structure of separatrices. The full system, written in terms of the variables $p,q,\ z\ ,\ \theta = \psi_2$, is of the form

$$\begin{aligned} d/dt\ (p,q) &= (-H_q(p,q,z)\ ,\ H_p(p,q,z)) + \epsilon\ (\ P_1(p,q,z,\theta),\ P_2(p,q,z,\theta)\ ) \\ dz/dt &= \epsilon\ R(p,q,z,\theta) \\ d\theta/dt &= S(p,q,z) + 0(\epsilon) \quad . \end{aligned} \tag{10.4}$$

Here γ_1 , γ_2, R_1, R_2 are assumed to be $0(\epsilon)$ and

$$\epsilon P_1 = -p[\gamma_1 + R_1 \sin(\theta + \varphi)]$$

$$\epsilon P_2 = -R_1 \cos(\theta + q) + R_2 \cos\theta$$

(10.5)

$$\epsilon R = -(\gamma_2 + R_2 \sin\theta)z - (p/S_{12})[\gamma_1 - \gamma_2 + R_1 \sin(\theta+q) - R_2 \sin\theta]$$

$$S = -\Delta_2 + p[-S_{21}\cos q + S_{21} S_2/S_{12} - T_{21}] - S_2 S_{21} z .$$

Wiggins, Holmes and Shaw [WiH,WiSh] studied systems of type (10.4), with S=1, using Melnikov's method. Their model is an "oscillator" (p,q) with a slowly varying parameter z and time periodic forcing $d\theta/dt = 1$. The fact that here S is not constant brings some technical difficulties only in case it changes sign, but the method of Melnikov can still be applied. Then some extra work is needed to insure the desired homoclinic behavior (S.Wiggins, personal communication) .

The calculations become remarkably simple for the symmetrical model [NOK], for which $\Delta_1 = \Delta_2 (= \Delta)$, $S_1 = S_2 (= S)$, $T_{12} = T_{21}$, $S_{12} = S_{21}$. Denoting $\alpha = S_2 - T_{12} = S_1 - T_{21}$ and taking units so that $S_{12} = S_{21} = 1$,

(10.6) $$H = p(p-z)(-\alpha + \cos q)$$

Phase portraits of (10.6) bifurcate at $\alpha = \pm 1$. See Fig.10.1a for the case $\alpha > 1$. The separatrices, energy level curves $H = h = z^2(\alpha - 1)/4$, are given by elementary functions, solving

$$dp/dt = \pm (\alpha^2-1)^{1/2} \, |p-(z/2)| \, [(p_+-p)(p-p_-)]^{1/2}$$

(10.7)

$$p_\pm = (z/2)\{1 \pm [(2/(\alpha+1)]^{1/2}\}$$

and extracting q(t) from (10.6).

The case $\alpha=0$ is specially simple (Fig.10.1b). Here

C_1: $p\# = 0$, $q\# = -\arcsin(\tgh\, zt)$
C_3: $p\# = z$, $q\# = \arcsin(\tgh\, zt)$

(10.8)

C_2: $q\# = \pi/2$, $p\# = z/(1+\exp(zt))$
C_4: $q\# = -\pi/2$, $p\# = z/(1+\exp(-zt))$

The Melnikov function M measures the distance, between stable and unstable invariant manifolds, for the perturbed system in the full phase space (p,q,z,θ). It is described geometrically as follows. For $\epsilon = 0$, the (p,q) dynamics decouple, z is constant, and

$$\theta^{\#}(t) = \theta_0 + \int_0^t S\,(\,p\#(t),\, q\#(t)\,,\, z_0\,)\,dt \tag{10.9}$$

where $x\#(t) = (\,p\#(t),\, q\#(t);\, z_0\,)$ is a separatrix of (10.2). Denote an unstable equilibrium of $H(p,q;z)$ by $x_\infty = (p_\infty(z),\, q_\infty(z))$ and by

$$M_0 = \bigcup_z x_\infty(z) \times \{\,(z,\theta)\,\}$$

the unperturbed normal manifold. For the sake of notation simplicity we are considering an homoclinic saddle point $x_\infty = \lim_{t \to \pm\infty} (p\#(t),\, q\#(t)\,)$ but everything holds true for heteroclinic connections.

For ϵ sufficiently small there is an invariant manifold M_ϵ, ϵ-close and a graph over M_0. M_ϵ has stable and unstable manifolds $W_\epsilon^{\,s,u}$. Their $0(\epsilon)$ distance can be measured (as depicted in Fig.10.2) by

$$M(a,z_0,\theta_0;\,\epsilon) = (\,\mathrm{grad}_{\,x\#(a;\,z_0)}\, H(x,z) \mid x_\epsilon^{\,u} - x_\epsilon^{\,s}\,) = \tag{10.10}$$

$$= \epsilon\, M_1(a,z_0,\theta_0) + 0(\epsilon^2)$$

where $a \in (-\infty,\infty)$ parametrizes the unperturbed separatrices and $x_\epsilon^{\,s,u}$ are the intersections of $W_\epsilon^{\,s,u} \cap \{z = z_0\,,\, \theta = \theta_0\}$ with the line L_a normal to the unperturbed separatrix at $x\#(a,z_0)$. In Appendix 4 we derive, in a slightly more general setting, the Melnikov formula

$$M_1(a,z_0,\theta_0) = \int_{-\infty}^{\infty} dt\,\Big(\,\mathrm{grad}\, H\,(x\#(t+a),z_0) \mid P(\,x\#(t+a,z_0,\theta^{\#}(t)) + \tag{10.11}$$

$$+ J\,H_{xz}(x\#(t+a),z_0) \int_0^t du\; R(u+a,z_0,\theta^{\#}(u))\,\Big)$$

where $J\,H_x = (-H_q\,,\, H_p\,)$. Here $\theta^{\#}$ is given by (10.9) with $x\# = x\#(t+a)$.

It follows from (10.10) that the sign of M_1 determines in which way $W_\epsilon^{\,u}$ and $W_\epsilon^{\,s}$ split apart. M_1 vanishes along trajectories of the unperturbed

system which "shadow" the doubly assymptotic solutions of the perturbed system as $\epsilon \to 0$. The union of these double asymptotic, or homoclinic curves, forms $W_\epsilon{}^u \cap W_\epsilon{}^s$.

The results of the computations, using the symmetric model with $\alpha = 0$ as in Fig.10.1b , and $\rho_1 = \rho_2 = 1$, $\gamma_1 = \gamma_2$ ($= \gamma$) are as follows:

$$
\begin{aligned}
&M_1 = 0 \\
&M_2 = A(z_0) \sin [\, \theta_0 + (\Delta + S\, z_0)a \, + \pi/4] \\
&M_4 = A(z_0) \sin [\, \theta_0 + (\Delta + S\, z_0)a \, - \pi/4 \,] \\
&M_3 = -\, \gamma\, (2\pi + z_0) + (R/\sqrt{2}\,)\{\, B(z_0) \cos \beta + C(z_0) \sin \beta \,\}
\end{aligned}
\tag{10.12}
$$

where

$$
\beta = \theta_0 + (\, \Delta + S\, z_0\,)a \, + 2 \arctan \exp(z_0 a)
\tag{10.13}
$$

$$
A(z_0) = \int_{-\infty}^{\infty} dt \, \{\cos\, (\Delta + S\, z_0)/\, \cosh^2(z_0 t/2)\, \}
\tag{10.14}
$$

$$
\begin{aligned}
B(z_0) = &\int_{-\infty}^{\infty} dt\{\operatorname{sech}^2(z_0 t)\tanh(z_0 t)\sin[(\Delta + S z_0)t + 2\operatorname{arctg}(\exp z_0 t - \pi/4)]\} \\
&+ \int_{-\infty}^{\infty} dt \operatorname{sech}(z_0 t)\tanh(z_0 t) \int_0^t du\, \{\cos[\arcsin\tanh(z_0 u) - u(\Delta + S z_0) \\
&\qquad - 2\operatorname{arctg}(\exp z_0 u - \pi/4)\,\}
\end{aligned}
\tag{10.15}
$$

$$
C(z_0) = \int_{-\infty}^{\infty} dt\, \{\operatorname{sech}(z_0 t)\tanh(z_0 t)\sin[(\Delta + S z_0)t + 2\operatorname{arctg}(\exp z_0 t - \pi/4)]\}
\tag{10.16}
$$

Although (10.14-16) could be explicitly evaluated by residues, this is not necessary for our purposes. Indeed, the necessary recurrence for homoclinic behavior follows directly from (10.12):

Proposition 10.1. Let C_i, i=1,...,4 the unperturbed separatrices (10.8) (Fig.10.1b). Then under the $O(\epsilon)$ perturbation, C_1 does not split, C_2 and C_4 *always* split with transversal intersections. C_3 splits with transversal intersections *provided* the ratio δ/R is not too large. Due to the presence of Smale horseshoes, there are infinitely many countable periodic motions of arbitrary high period and infinitely many uncountable bounded non-periodic chaotic motions.

Remarks . (i) The calculations were done for $\alpha=0$, value at which the topology of the unperturbed phase portraits changes (Fig.10.1). It is physically reasonable that for small $\alpha\neq0$, a sufficiently large ϵ will create, around the *two* unperturbed separatrices given by $\cos q = \alpha$, a *single* stochastic layer. (ii) Simultaneous zeros of the first and second Melnikov functions yield *homoclinic tangencies* . The formula for M_3 in (10.12) shows that this happens for a certain value as δ/R increases. Homoclinic tangencies provoke interesting dynamical consequences, including infinitely many attracting periodic orbits and cascades of period doublings [P,PT]. It would be interesting to investigate numerically the ocurrence of these phenomena. The formula for M_3 also indicates that when δ/R surpasses a certain critical value, then it is possible that homoclinic chaos ceases to occur. (iii) For larger values of the perturbation parameters R and δ, it is expected that the "mild chaotic" orbits of Proposition 10.1 will evolve into strange attractors with fractional dimensions.

11. Further topics for research.

Besides those already discussed in previous sections, we present the following.

Families of equilibrium solutions . There are only a finite number of equilibria for any choice of parameters: since the system can be written as a set of quadratic ODEs in R^6, Bezout's lemma implies that there are exactly 2^6 complex solutions, counting multiplicities (certainly much less real physical solutions; the same counting for the C-equations gives 3^4). In comparison, Lorenz's system has at most three distinct real solutions among the 2^3 complex. We have shown that several equilibria may coexist for certain parameter ranges: besides the origin and the branch described in §7, there are two solutions with $n_2=0$, and two with $n_1=0$. From each of these, strong-weak pairs can bifurcate.

In the symmetrical case (§7), other equilibrium solutions with $n_1 \neq n_2$ may emanate out from the $n_1=n_2$ branch, via the center manifold theorem, at the control parameter values where there is a zero eigenvalue. This brings up the following conjecture: the emanating branches *connect* with those which arise from the $n_1=0$, $n_2 \neq 0$ ($n_2 \neq 0$, $n_1 \neq 0$) solutions in §5. We plan to pursue this study by path following methods, using codes such as AUTO or PITCON [Do, Rh].

In the asymmetrical case find, e.g. via Routh-Hurwitz type criteria, values of h for which J changes stability. Is it possible that Hopf bifurcations take place? More generally, is it possible to give a complete description of all equilibrium point branches of the two-mode system, and their stability classification?

Comparisons with Lorenz's equations . While the Lorenz system has only three parameters, the number of parameters of the 2-mode spin-wave system is 10 (or 12 if one allows asymetric values $S_{12} \neq S_{21}$ and $T_{12} \neq T_{21}$). Lorenz's system is known to possess Liapunov functions, for any choice of the parameters, so all motions tend to bounded regions. It would be interesting to find Liapunov functions for the spin-wave system, at least for certain ranges of parameters (the Hamiltonian is a natural candidate). We showed in section 4 that for special parameter values escapes to infinity are possible.

Lorenz's system has at most three equilibrium points. The origin of Lorenz's strange attractor is identified to a "homoclinic explosion", a *global*

bifurcation due to homoclinic and heteroclinic connections between the three equilibrium points [Sp], which occur frequently as the parameters are varied (usually r is taken as the control parameter). These critical values of the parameters have been found numerically through extensive studies done by several research groups. For the spin-wave system, can one establish recurrent homoclinic connections between the unstable equilibria (the so-called "cycles" [PBMB]) at certain parameter values? One may exploit the symmetry properties of the C-equations to classify, by combinatorial arguments, the global structure of the homoclinic bifurcations [Gl].

On the nearly hamiltonian limit . For N≥3 modes without dissipation, are there additional constants of motion for specific choices of parameters, yielding "accidental" integrable cases (i.e, without symmetries)? This study could be attempted via Kowalevskaya-Painleve's analysis.

The three mode system with zero dissipations and pumping and can be reduced to a two degrees of freedom Hamiltonian. Find the relative equilibria with three modes, and their stability. Assuming initial conditions where one of the modes is weak (say, $n_3<<1$), will it remain weak? Can it induce Arnold's diffusion on the other two modes?

Given a nearly integrable Hamiltonian system with dissipation terms added, can one describe the process of transition from the usual KAM situation to the appearance of strange attractors with non-vanishing fractal or Hausforff dimensions? This question is related to an idea proposed by Smale [Sm]: "I would like to develop the idea that by introducing a dissipation/forcing term into Hamilton's equations of physics, one might be able to revive the ergodic hypothesis of Boltzmann and Birkhoff".

12. Discussion.

Summary . We have shown that the spin-wave S-equations of Zakharov and collaborators [ZLS], using the Cooper-pair variables, are mathematically equivalent to the model used by Jeffries and co-workers [BJN] for perpendicular pumping (C-equations). The latter are well behaved at the origin and have nice symmetry properties; nevertheless, we have chosen to use Zakharov's equations, mainly because emphasis in this work is given to the bifurcations ocurring "far" from the origin. Moreover, the Cooper-pair variables have a nice physical interpretation.

We have identified the mechanisms leading to nonzero steady states and Hopf bifurcations. It would certainly be interesting to make the analysis directly on an infinite-dimensional evolution equation, e.g. Landau-Lifshitz equation with dissipation included. We have discussed two new organizing centers for routes to chaos, namely a codimension-2 bifurcation (with one zero real eigenvalue and two imaginary ones) and the Hamiltonian limit with nearly zero dissipation.

Analogies with other physical systems . Kovacic and Wiggins studied a two mode truncation of the forced and damped Sine-Gordon equation; an intermediate step leads to a nonlinear Schrodinger equation. Their model [KW,$(1.3)_\epsilon$] is precisely the C-equations with a special choice of parameters, except for the forcing, which there is a constant term. Thus we believe that the C-equations have a "universal nature".

Suhl's often quoted observation [S, 1957] that spin-wave instabilities "resemble turbulent motion in fluid mechanics", prompt us to inquire if this analogy can be carried further. Recall that Lorenz's equations, probably the most widely studied dynamical system [Sp,Sp1], models a two-dimensional fluid cell warmed from below and cooled from above. The resulting PDE is truncated into a set of three modes, pruducing a set of three coupled ODEs with quadratic nonlinearities, depending on three positive parameters r, b, σ : $x' = \sigma(y-x)$, $y' = rx - y - xz$, $z' = -bz + xy$. We saw that the spin-wave system can also be written as a dynamical system with *quadratic* nonlinearities, but for N modes it is necessary to extend the phase space to 3N-dimensions. Like the Lorenz system, the flow is dissipative (volume contracting), with *constant* negative divergence.

Holmes [H1] found homoclinic bifurcations on a model for weakly nonlinear surface waves on a closed basin. Based on earlier work by Miles [Mi], the system consists of a two degree of freedom Hamiltonian with dissipation

$$q_1' = -(\Delta+3/4\ e)\ p_1 + m\ q_2 + \alpha - \gamma\ q_1$$
$$p_1' = (\Delta+3/4\ e)\ q_1 + m\ p_2 - \gamma\ p_1$$
$$q_2' = -(\Delta+3/4\ e)\ p_2 - mq_1 - \gamma\ q_2$$
$$p_2' = (\Delta+3/4\ e)\ q_2 - mp_1 - \gamma\ p_2$$

The Hamiltonian is

$$H = -1/2\ (\Delta+3/8\ e)e + m^2 + \alpha\ p_1$$

with

$$e = q_1^2 + p_1^2 + q_2^2 + p_2^2 \quad , \quad 2m = p_1q_2 - q_1p_2 \ .$$

More recently, Kambe and Umeki [KU] studied the system (also based on Miles' theory) $(d/dt + \gamma_i)\ (p_i,q_i) = (-\partial/\partial q_i,\ \partial/\partial p_i)\ H$, i=1,2, with

$$H = 1/2\ \Sigma_{i=1,2}\ [A_o(p_i^2-q_i^2) + \beta_i(p_i^2+q_i^2) + 1/2\ A_i\ (p_i^2+q_i^2)^2] +$$

$$+ 1/2\ C\ (p_1^2+q_1^2)(p_2^2+q_2^2) + 1/2\ D\ (p_1q_2-p_2q_1)^2$$

These authors show that here the main bifurcations are not of homoclinic type. We observe that both sets of equations are similar to the C-equations for spin-waves, namely, with linear and cubic terms. We believe that for the spin-wave system, both homoclinic bifurcations near the Hamiltonian limit and other, more typically dissipative bifurcations, may describe observable physical phenomena.

In another tack, Mirollo and Strogatz [MS] have studied the *gradient* system $d\theta_k/dt = -\partial H/\partial\theta_k$, $1 \le k \le N$, where the potential function H is

$$H = -\Sigma_k\ \cos(\beta_k - \theta_k) - K/2N\ \Sigma_{k,k'} \cos\ (\theta_k-\theta_{k'}).$$

Physically, a random pinning field tries to "pin" each θ_k at a random angle β_k , counteracted by an attractive interaction between the phases. The β_k are uniformly distributed random variables in the unit circle. The equilibria undergo jump bifurcations and hysteresis as the parameter K varies. Similarly, jump bifurcations and hysteresis are present in spin-waves.

Onset of auto-oscillations . In a footnote on [ON,p.L607], a remark is made that the asymmetrical solutions $n_1 \neq 0$, $n_2 \neq 0$, with $n_1 \neq n_2$, $n_2 << 1$ "are not analytically tractable". However, these solutions are precisely those analytically studied in §6, where we have shown the ocurrence of Hopf bifurcations (followed in many cases by cascades of period doublings). These strong mode-weak mode equilibrium solutions seem to be the relevant ones to describe the onset of auto-oscillations in the physical experiments. In fact, for the symmetrical case we have shown that no Hopf bifurcations occur on the branch $n_1 = n_2$. A comparison with the work by Zhang and Suhl [ZS] is perhaps in order. Equation (6) of that paper with $B_k = C_k$, $\zeta_k = 0$ and $\rho_{kk'} = - i S_{kk'}$ is $dc_k/dt = - \eta\ c_k - i \omega_s V_k c^*_{-k} - \Sigma_k S_{kk'} c_{k'} c_{-k'} c^*_{-k}$ (ζ represents a thermal value; in the numerical solution a initial value $\neq 0$ plays the role of thermal fluctuation). Making $\eta = \gamma_k$ and $\omega_s V_k = h \rho_k$, this equation becomes identical to (2.12) with $\Delta\omega_k = T_{kk'} = 0$, and where $S_{kk'}$ is pure imaginary. With these constraints Zhang and Suhl obtain auto-oscillations independently of choice of the other parameters. Notice however, that in [ZS] these authors report that in some experiments "the auto-oscillation frequency is found to be of the same order as damping". Unless one assumes all coefficients to be proportional to damping, this seems not in agreement with a prediction for the frequency based on §6. Our result for the frequency is the imaginary part for the eigenvalue pair of the strong mode (as an isolated system) plus a correction of the same order as the damping.

Modified spin-wave equations . It was shown in [RACK] that when the two modes participating in the interaction are close, i.e, $k_1 - k_2 = \pi/d$ where d is the sample width, one must add "∂ terms" to equations (2.12) and the modes become coupled *already* in the linear approximation:

$$dc_1/dt = - (\gamma_1 + i\Delta\omega_1)c_1 - i R_1 (c_1^* - i \partial_1 c_2^*) - \text{terms in S and T}$$
$$dc_2/dt = - (\gamma_2 + i\Delta\omega_2)c_2 - i R_2 (c_2^* - i \partial_2 c_1^*) - \text{terms in S and T}$$

Numerical experiments, which will be reported elsewhere, indicate that substantially different dynamic behavior occurs; a theoretical study is definitely in order. We predict a sample size dependence on the frequency of auto-oscillations, more in accordance with the physical experiments.

Appendix1. Stability of equilibrium ($n_1 \neq 0, n_2 = 0$) when $A^2+B^2 < C^2$

Let's recall some well known facts of Floquet's theory. The stability of a periodic orbit is determined by the eigenvalues of the monodromy matrix M(T) associated to the linearization along that periodic solution. These eigenvalues are here functions of the control parameter h. One multiplier is always equal to 1; if some other multiplier crosses the unit circle, the periodic orbit becomes unstable. Three cases are possible: first, if the crossing is at some non real number then, generically, a Hopf bifurcation on the Poincaré map of a transverse section takes place, and an invariant torus is born. The other possibilities are real multipliers passing through ± 1. The -1 case is generically related to a period doubling bifurcation, while the +1 case to the collision of a stable with an unstable family of closed orbits, desappearing after surpassing the corresponding control parameter value.

None of these possibilities occur in (5.6): the periodic orbit remains stable as long as $A^2+B^2 < C^2$. This result can be proven indirectly: since in the C-representation the periodic orbit appears as an equilibrium point, it would suffice to study its stability. We prefer to give a direct proof.

The monodromy matrix satisfies the linear T-periodic system $dM/dt=JM$, $M(0)=id$, where J is as in (5.11) and Table 1. Here ψ_2^e (which does not exist in this case) is replaced by the periodic function $\psi_2(t)$, solution of (5.7). Denote by Δn_1 , $\Delta\psi_1$, Δn_2 , $\Delta\psi_2$ the linearized variables. It follows from the above linear ODE $M=J(t)M$ that the structure of M(T) is as follows:

$$M(T) = \begin{pmatrix} & & m_{13} & 0 \\ \exp(J_{(2)}T) & & m_{23} & 0 \\ 0 & 0 & \mu & 0 \\ m_{41} & m_{42} & m_{43} & 1 \end{pmatrix} \qquad \text{(A1.1)}$$

Consequently, the multipliers are 1, μ, and the exponentials of the eigenvalues of the constant matrix $TJ_{(2)}$ where $J_{(2)}$ is given by (4.3). The latter two multipliers, therefore, have always modulus <1. Now $\Delta n_2/\Delta n_2 = \lambda_3(t)$ so that $\Delta n_2 (T) = \mu \Delta n_2(0)$ where

$$(A1.2) \qquad \mu = \exp\left(\int_0^T \lambda_3(t)\, dt \right) \geq 0$$

One observes on Table 2 that $\lambda_3 (t) = - \gamma_2 - \lambda_4 (t)$. Since from general principles

$$(A1.3) \qquad \int_0^T \lambda_4 (t)\, dt = 0$$

(this corresponds to the multiplier 1; if one is skeptic, this can be confirmed directly by a long calculation using residues), one concludes that

$$(A1.4) \qquad 0 \leq \mu = \exp (-\gamma_2 T) \leq 1 .$$

The periodic orbit is *stable* as long as it exists, ie., as long as $A^2+B^2 < C^2$.

Appendix 2. A center manifold calculation (by Prof.Richard Rand).

As one moves along branch L^s of equilibrium points, varying the control parameter h, there is a value h^* at which λ_3 changes from negative to positive. At this moment a center manifold with $n_2 \neq 0$ is born. This center manifold, and the flow on it, was calculated to second order, using MACSYMA, by Professor Richard H. Rand, of Cornell University.

Let's describe the main steps of the calculation. At an equilibrium point we know the eigenvalues and the matrices P, P^{-1} that change to a suitable eigenvector basis (Proposition 5.2). So we get a new system of coordinates u_1, u_2, u_3, u_4 relative to the eigenbasis, centered at the equilibrium point. The coordinate n_2 corresponds basically to u_1.

Following an idea exposed in [C], an additional variable $u_0 = h - h^*$ is introduced. Thus, for instance, what was a linear term like hu_1 becomes now $hu_1 = u_0 u_1 + h^* u_1$, that is, a quadratic term plus a linear term.

Making a Taylor expansion of n_1, ψ_1, n_2, ψ_2 and a, b, c, d, e (the latter are terms of the matrix P) with respect to u_0 , one gets a new system of ODEs for u_i , $0 \leq i \leq 4$. Note that by construction,the constant terms that appear in these equations are zero. The structure is of the form

$$u_i = \sum_{j=0}^{4} (k_{ij} u_j + B_{ij} u_j^2) + \sum_{m=0}^{4} \left(\sum_{n=m+1}^{4} C_{imn} u_m u_n \right) \qquad \text{(A2.1)}$$

where the coefficients can be stored in "telescoping" archives, according to consecutive levels of complexity in terms of the original parameters.

Finally, it was applied the algorithm given by Rand and Ambruster [RHA], to obtain the center manifold and the flow on it, truncated at quadratic terms. The center manifold is given by

$$u_2 = (- B_{21} u_1^2 - C_{201} u_0 u_1 - B_{20} u_0^2)/ k_{22}$$

$$u_3 = -[(B_{41}k_{32} - B_{31}k_{44})u_1^2 + (C_{401}k_{34} - C_{301}k_{44})u_0 u_1 + (B_{40}k_{34} B_{30}k_{44})u_0^2]/k_{34}k_{43} \qquad \text{(A2.2)}$$

$$u_4 = (- B_{31} u_1^2 - C_{301} u_0 u_1 - B_{30} u_0^2)/ k_{34}$$

and the flow on it is

(A2.3) $$du_1/dt = B_{11}\, u_1^2 + C_{101}\, u_0 u_1 + 0(3)$$

One obtains the nonzero equilibrium

(A2.4) $$u_1 = - C_{101}\, u_0 / B_{11} + 0(u_0^2)$$

which in the case we are interested represents a transcritical bifurcation.

Appendix 3. Control parameter value for Hopf bifurcation.

Although there is no guarantee that $h_{Hopf} - h^*$ is small, the numerical experiment in section 6 suggests that a good prediction for h_{Hopf} can still be obtained truncating to first order. The Jacobian matrix at the equilibrium point in the center manifold is expanded about the parameter value h^* where this manifold is born:

(A3.1) $$J = J^* + (h-h^*)J_1 + O(h-h^*)^2 \cdot$$

Let μ^* the complex eigenvalue of J^* given by

(A3.2) $$\mu^* = -\sigma_1/2 + i \{ S_1 J_{12} - (\sigma_1/2)^2 \}^{1/2}$$

Expanding the perturbed simple eigenvalue and eigenvector as

$$\mu = \mu^* + (h-h^*)\mu_1 + O(h-h^*)^2 \ , \quad v = v^* + (h-h^*)v_1 + O(h-h^*)^2 \ ,$$

we get $J^*v^*=\mu^*v^*$ and $(J^*-\mu^*id)v_1 - \mu_1 v^* = -J_1 v^*$.

Taking the real inner product of this equation with the row-eigenvector w^* of J^* (also asssociated to μ^*), then $\mu_1 = (J_1 v^*, w^*) / (v^*,w^*)$.

It follows that taking first order truncations,

(A3.3) $$h_{Hopf} \approx h^* - Re\mu^*/Re\mu_1 = h^* + \sigma_1/(2Re\mu_1) \ .$$

This seems reasonable: we have assumed σ_1 to be small. Now, in order to compute $Re\mu_1$ we need v^*,w^* and J_1. We find readily

(A3.4)
$$v^* = (1, \mu^*/J_{12}, 0 , (J_{41} + J_{42}\mu^*/J_{12})/(\mu^*-\lambda_4))$$
$$w^* = (1,-\mu^*/T_1, J_{13}/\mu^* - J_{23}/T_1, 0).$$

The matrix J_1 is the directional derivative of the general Jacobian J, computed at h^*, in the direction of the center manifold equilibrium point (which is a linear function of $h-h^*$ in the first order theory). For this calculation the telescoping archives alluded to in Appendix 2 are needed.

Appendix 4. A Melnikov formula.

A general tratment can be found in Wiggins [Wi], but since the derivation is short we present it here for completeness. Write the curves $x_\epsilon{}^{u,s}(t)$ with initial conditions $(x_\epsilon{}^{u,s}(a;z_0),z_0,\theta_0)$ as

$$x^{u,s}(t) = x\#(t+a;\, z_0) + \epsilon\, \xi^{u,s}(t\,;a,z_0,\theta_0) + 0(\epsilon^2)$$

(A4.1) $$z^{u,s}(t) = z_0 + \epsilon\, \lambda^{u,s}(t\,;a,z_0,\theta_0) + 0(\epsilon^2)$$

$$\theta^{u,s}(t) = \theta^{\#}(t\,;\, a,z_0,\theta_0) + 0(\epsilon)$$

where $\theta^{\#}(t)$ satisfies the initial value problem

(A4.2) $$d\theta/dt = S(\, x\#(t+a);\, z_0,\theta_0)\,, \quad \theta(0) = \theta_0\,.$$

We take $\lambda^{u,s}(0) = 0$ so that initial conditions are in the z_0 level. Substituting (A4.1) into (10.4) one gets the equations of variation

(A4.3) $$d\lambda/dt = R(\, x\#,\, z_0,\, \theta^{\#})\,, \quad \lambda\,(0) = 0$$

(A4.4) $$d\xi^{\,s,u}/dt = J\,H_{xx}\,(\, x\#,z_0)\,\xi^{\,s,u} + J\,H_{xz}(x\#,z_0)\,\lambda + P(\, x\#,z_0,\theta^{\#}).$$

Here we have omitted the s,u superscripts in λ since it turns out that the same equation (A4.3) is satisfied for both. The initial values $\xi^{s,u}(0)$ are uniquely determined by the dichotomy condition $X^s(t) \to M_\epsilon$ as $t \to \infty$ and $X^u(t) \to M_\epsilon$ as $t \to -\infty$. Moreover, the solutions ξ^s (ξ^u) remain bounded as $t \to \infty$ ($t \to -\infty$) respectively. Substituting (A4.1) in the definition (10.10) we get $M_1(a,z_0,\theta_0) = \Delta^u(0) - \Delta^s(0)$ where

(A4.5) $$\Delta^{s,u}(t) = (\, \text{grad}\, H(\, x\#(t+a);z_0) \mid \xi^{s,u}(t\,;\, a,z_0,\theta_0)\,).$$

Furthermore

$$(A4.6)\quad \Delta^s(0) = -\int_0^{T_1} d/dt\ \Delta^s(t)\,dt + \Delta^s(T_1)$$

$$(A4.7)\quad \Delta^u(0) = \int_{-T_2}^{0} d/dt\ \Delta^u(t)\,dt + \Delta^u(-T_2)$$

where

$$(A4.8)\quad d/dt\ \Delta^{s,u} = (d^2_x H\ x \mid \xi^{s,u}) + (\text{grad } H \mid JH_{xx}\,\xi^{s,u})$$

$$+ (\text{grad } H \mid J H_{xz}\,\lambda + P).$$

The first two terms cancel out and $\Delta^s(T_1), \Delta^u(T_2) \to 0$ as $T_1, T_2 \to \infty$. The Melnikov formula (10.11) is therefore obtained.

Acknowledgements. We thank Professor R.H.Rand for providing the center manifold calculation and for pointing out the existence of the codimension-two bifurcation. We thank Professors S.Wiggins and P.J.Holmes for discussions on the near Hamiltonian limit. One of us (A.C.) wishes to thank the Brazilian agency CNPq for financial support; (J.K.) wishes to thank the Brazilian agency FAPERJ for financing a visit to MSRI, Berkeley.

References

[A] Arnol'd,V.I., Mathematical Methods of Classical Mechanics, Springer-Verlag, 1978.

[AAR] Aguiar,F.M., Azevedo, A., Rezende, S.M., Characterization of strange attractors in spin-wave chaos, Phys.Rev.B 39:13 (1989) 9448-9452.

[AM] Abraham, R., Marsden,J.E., Foundations of Mechanics, Benjamin, 1978.

[AR] Aguiar,F.M., Rezende, S.M., Observation of subharmonic routes to chaos in parallel-pumped spin waves in Yttrium Iron Garnet, Phys.Rev.Lett. 56:10 (1986), 1070-1073.

[BJN] Bryant,P., Jeffries,C., Nakamura,K., Spin-Wave turbulence, Nuclear Phys.B (Proc.Suppl.) 2 (1987) 25-36.

[BJN1] Bryant,P., Jeffries,C., Nakamura,K., Spin-Wave nonlinear dynamics in an Yttrium Iron Garnet Sphere, Phys.Rev.lett. 60:12 (1988), 1185-1188.

[BJN2] Bryant,P., Jeffries,C., Nakamura,K., Spin-wave dynamics in a ferrimagnetic sphere, Phys.Rev.A 38:8 (1988), 4223-4240.

[C] Carr, J., Applications of Center Manifold Theory , Springer-Verlag, 1981.

[CDF] Chow, S.N., Deng, B., Fiedler, B., Homoclinic bifurcation at resonant eigenvalues, J.Dyn. Diff. Eqs. 2:2 (1990) 77-244.

[CRP] Carrol, T.L., Rachford, F.J., Pecora, L.M., Ocurrence of chaotic transients during transitions between quasiperiodic states in yttrium iron garnet, Phys. Rev. B 38:4 (1988) 2938-2940.

[CSG] Carr,J., Sanders, J., van Gils, S., Non resonant bifurcations with symmetry, SIAM J. Math. Anal. 18:3 (1987) 579-592.

[De] Deng, B., Homoclinic bifurcations with nonhyperbolic equilibria, SIAM J. Math. Anal. 21:3 (1990), 693-720.

[DL] Dressler,U., Lauterborn, W. , Ruelle's rotation frequency for a symplectic chain of dissipative oscillators, Phys. Rev. A 41:12 (1990) 6702-6715.

[Do] Doedel, E. , Computer code AUTO, Pasadena, CA.

[Dr] Dressler, U., Symmetry property of the Lyapunov spectra of a class of dissipative dynamical systems with viscous damping, Phys. Rev.A 38 (1988), 2103-2109.

[GH] Guckenheimer, J., Holmes, P., Nonlinear Oscillations, Dynamical Systems, and Bifurcations of Vectorfields, Springer-Verlag, 1983.

[GJ] Gibson, G., Jeffries, C., Observation of period doubling and chaos on spin-wave instabilities in yttrium iron garnet, Phys.Rev.A 29:2 (1984) 811-818.

[Gl] Glendinning, P., Global structure of homoclinic bifurcations: a combinatorial approach, Phys.Lett.A 141:8/9 (1989), 391-396.

[GL] Glazier, J.A., Libchaber, A., Quasi-periodicity and dynamical systems: an experimentalist's view, IEEE Trans.Circuits Systems 35:7 (1988) 790-807.

[GZ] Gill, T.P., Zachary, W.W., Number of modes governing spin-wave turbulence, J.Appl.Phys. 61:8 (1987), 4130-4132.

[H] Holmes, P., Periodic, nonperiodic and irregular motions in a Hamiltonian system, Rocky Mountain J.Math. 10:4 (1980) 679-693.
[H1] Holmes, P., Chaotic motions in a weakly nonlinear model for surface waves, J.Fluid Mech., 162 (1986) 365-388.
[HPW] Hartwick, T.S., Peressini, E.R., Weiss, M.T., Subsidiary resonance in YIG, J.Appl. Phys. 32S (1961) 223S-224S.
[JB] Jeffries,C.D., Bryant,P.H., Nonlinear dynamics of spin waves, J.Appl.Phys. 64:10 (1988) 5382-5385.
[K] Keffer, F., Spin Waves, in Handbuch der Physik vol.XVIII/2, ed. by S.Flügge, Springer Verlag, 1966.
[Kap] Kapitaniak, T., Analytical condition for chaotic behavior on the Duffing oscillator, Phys.Lett.A 144:6/7 (1990), 322-324.
[Ke] Keener, J.P., Oscillatory coexistence in the chemostat: a codimension two unfolding, SIAM J. Appl. Math. 43:5 (1983) 1005-1018.
[Ke1] Keener, J.P., Infinite period bifurcation and global bifurcation branches, SIAM J. Appl. Math. 41 (1981) 127-144.
[KM] Kubicek, M., Marek, M., Computational Methods in Bifurcation Theory and Dissipative Structures , Springer Verlag, 1983.
[KU] Kamke,T., Umeki, M., Nonlinear dynamics of two-mode interactions in parametrically excitation of surface waves, J.Fluid Mech. 212 (1990), 373-393.
[KW] Kovacic, G., Wiggins, S., Orbits homoclinic to resonances: chaos in a model of the forced and damped sine-Gordon equation, to appear in Arch. Rat. Mech. Anal.
[LH] Lin, S.P., Huber, D.L., Instabilities of spin waves in parallel-pumped easy plane ferromagnets, J.Appl. Phys. 63:8 (1988) 4151-4153.
[Li] Ling, T.H., On the Melnikov method, ZAMM 67:4 (1987) T107-109.
[M] Morgenthaler, F.R., Survay of ferromagnetic resonance in small ferrimagnetic ellipsoids, J.Appl.Phys.31 (1960) 95S- 97S.
[Mi] Miles, J.W., Nonlinear surface waves in closed basins, J.Fluid Mech. 75 (1976), 419-448.
[MS] Mirollo R., Strogatz, S., Jump bifurcation and hysteresis in an infinite-dimensional dynamical system of coupled spins, SIAM J. Appl. Math., 50:1 (1990), 108-124.
[MW] McMichael, R.D., Wigen, P.E., High-power ferromagnetic resonance without a degenerate spin-wave manifold, Phys. Rev. Lett. 64:1 (1990) 64-67.
[NOK] Nakamura,K., Ohta,S., Kawasaki,K., Chaotic states of ferromagnets in strong parallel pumping fields, J.Phys, C: Solid State Phys. 15 (1982) L143-L148.
[OCR] Ozório de Almeida, A.M., Coutinho, T.J.S.B., Ritter, G.L.da Silva, Analytic Determination of Homoclinic Points in Chaotic maps, Rev.Bras.Fisica, 15:1 (1985), 60-69.

[ON] Ohta,S., Nakamura, K., Power spectra of chaotic states in driven magnets, J.Phys.C: Solid State Phys. 16 (1983) L605-L612.
[OV] Opheusden, H.J., Valkering, T.P., Period-doubling density waves in a chain, Nonlinearity 2 (1989) 357-372.
[P] Palis, J., Homoclinic orbits, hyperbolic dynamics and dimension of Cantor sets, Contemporary Math. 58:3 (1987) 203-216.
[PBMB] Pacifico, M.J., Bamon, R., Mañe, R., Labarca, R., Bifurcating simple vectorfields through singular cycles, preprint, IMPA/Br, 1990.
[PT] Palis, J., Takens, F., Homoclinic bifurcations and Hyperbolic dynamics, Cambridge Univ.Press, to appear.
[RA] Rezende,S.M., Aguiar, F.M., Strange Attractors in Spin-Wave Chaos, Physica A 163 (1990) 232-247 .
[RA1] Rezende,S.M., Aguiar, F.M., Nonlinear dynamics and chaotic behavior of spin wave instabilities, Rev. Bras. Fis. 16 (1986) 324-357.
[RAA] Rezende, S.M., Aguiar, F.M., Azevedo, A., Spin-wave auto-oscillations still in need of a good model, J.Appl. Phys. 67:9 (1990), 5624-5629.
[RACK] Rezende, S.M., Azevedo, A., Cascon, A., Koiller, J., Organizing center of bifurcations in spin-wave instabilities, Proc. Conf. Magnetism and Magnatic Materials, San Diego, 1990, to appear in J.Appl. Phys.
[Rd] Rand,R., Analytical approximation for period-doubling following a Hopf bifurcation, Mech, Res. Commun. 16:2 (1989) 117-123.
[Rh] Rheinboldt, W.C., Numerical analysis of parametrized nonlinear equations, Wiley, 1986.
[RHA] Rand, R.H.,Armbruster, D., Perturbation methods, bifurcation theory and computer algebra, Springer-Verlag, 1987.
[Ro] Roberts, A.J., The utility of an invariant manifold description of the evolution of a dynamical system,SIAM J.Math. Anal. 20:6 (1990), 1447-1459.
[ROD] Ritter, G.L. da Silva, Ozório de Almeida, A.M., Douady, R., Analytical determination of unstable periodic orbits in area preserving maps, Physica 29D (1987), 181-190.
[S] Suhl. H., Origin and use of instabilities in ferromagnetic resonance, J.Appl.Phys. 29:3 (1958) 416-421 (see also Suhl, H., J.Phys. Chem. Solids 1 (1957) 209).
[SGM] Schlomann,E., Green, J.J., Milano, V., Recent developments in ferromagnetic resonance at high power levels, J.Appl. Phys.31(1960) 386S-395S.
[Si] Silnikov, L.P., Some cases of generation of periodic motions in an n-dimensional space, Sov.Math.Dokl. 6 (1962), 163-166.
[Si1] Silnikov, L.P., On the generation of periodic motion from trajectories doubly asymptotic to an equilibrium state of saddle type, Math. USSR Sb. 6 (1968), 427-437.

[Sm] Smale, S., On the problem of reviving the ergodic hypothesis of Boltzmann and Birkhoff, in Smale, S., The Mathematics of Time , Spinger-Verlag, 1980, 137-144.
[Sp] Sparrow, C., The Lorenz equations: Bifurcations, Chaos, and Strange Attractors, Springer-Verlag, New York, Heildelberg, Berlin, 1982.
[Sp1] Sparrow,C., The Lorenz equations, in Holden, A.V., ed., Chaos, Manchester Univ.Press, Manchester, 1986.
[SZ] Suhl,H., Zhang, X.Y., Spatial and temporal patterns in high power ferromagnetic resonance, Phys. Rev. lett. 57:12 (1986), 1480-1483.
[VDG] Valkering. T.P., Derks, G., Groesen, E., in Singular behavior and Nonlinear Dynamics, ed by Bountis,T., St. and Sp.Pnevmaticos, World Sci., 1988.
[YM] Yamazaki,H., Mino,M., Chaos in Spin-Wave Instabilities,Progr.Theor.Phys. (supplement) 98 (1989), 400-41.
[YMNW] Yamazaki, H., Mino, M., Nagashima, H., Warden, M., Strange attractor of chaotic magnons observed in ferromagnetic $(CH_3NH_3)_2CuCl_4$, J. Phys. Soc. Japan 56 (1987) 742-750.
[W] White, R.M., Quantum theory of Magnetism, Springer-Verlag, 1983.
[Wa] Waldner, F., A 'stroboscopic model' for non-linear ferromagnetic resonance phenomena, J.Phys.C:Solid State Phys.21 (1988) 1243-1255.
[WBY] Waldner, F. , Barberis, D.R. , Yamazaki, H. , Route to chaos by irregular periods: simulations of parallel pumping in ferromagnets, Phys. Rev.A 31:1 (1985) 420-431.
[Wi] Wiggins, S., Global bifurcations and chaos: analytical methods, Springer, 1988.
[WiH] Wiggins, S., Holmes, P., Homoclinic orbits in slowly varying oscillators, SIAM J.Math. Anal., 18:3 (1987) 612-629, 19:5 (1988) 1254-1255.
[WiSh] Wiggins, S. Shaw, S.W., Chaos and three-dimensional horseshoes in slowly varying oscillators, J.Appl.Mech. 55 (1988) 959-968.
[WS] White, R.M., Sparks, M., Ferromagnetic relaxation. III. Theory of instabilities, Phys. Rev. 130:2 (1963) 632-638.
[ZLS] Zakharov,V.E., L'vov,V.S., Starobinets,S.S.,Spin-wave turbulence beyond the parametric excitation threshold, Sov.Phys.Usp.17 (1975),896-919.
[ZS] Zhang,X.Y., Suhl,H., Spin-wave related period doublings and chaos under transverse pumping, Phys. Rev.A 32:4 (1985) 2530-2533.
[ZS1] Zhang,X.Y., Suhl,H., Theory of auto-oscillations in high power ferromagnetic resonance, Phys. Rev.B 38:7 (1988) 4893-4905.

Figure captions

Fig.2.1. Dispersion relation: a.parallel pumping; b. perpendicular pumping.

Fig. 4.1. Nonzero equilibria for 1-mode system. Hysteresis occurs in cases b) and d).

Fig. 4.2. Phase portrait for a 1-mode system. Δ=1. , T=-1. , R=1.2 ($\Box$ = spiral sink; $\boxplus$ = node sink ; $\oplus$ = saddle).

Fig. 6.1. Hopf bifurcation: projections to (n_1,n_2) plane. For $1.0 \le R \le 2.4$, the "strong mode" n_1 is alone. When R exceeds 2.4, a center manifold with $n_2 \neq 0$ ("weak mode") is born. At R=3.15, a Hopf bifurcation into a limit cycle occurs. The parameters are the following, using equation (2.16): α = 0.7, g =5.0, $\Delta_1=\Delta_2$ = 0, $S_{11}+2T_{11}=-1$, $S_{22}+2T_{22}$ = 0.5, S_{12} = 2.5 and T_{12} = 1.125.

Fig. 6.2. Hopf bifurcation: trajectories of the eigenvalues of the Jacobian matrix in the complex plane for the parameters as in Fig.6.1.

Fig. 6.3. Amplitude of oscillations on a physical experiment, corresponding to a Hopf bifurcation (taken from [RACK]).

Fig. 7.1. Symmetrical case: family of periodic solutions. In the notations of (2.16), γ_i=1, Δ_i= -1, $S_{ii}+2T_{ii}$=1 , T_{12}= -0.75, S_{12}=-0.4.

Fig. 8.1. Heteroclinic phenomena at the origin: "pseudo" Silnikov's case. In the notations of eq. (2.12), $\gamma_1=\gamma_2$=1 , $\rho_1=\rho_2$=1, Δ_1= -1.384, Δ_2= 1.254, $S_1+2T_1 = S_2+2T_2$ = -0.286, S_{12} = 4.078, T_{12}=0. For mode 1 we get h^1_{fn}= 1.884 , h^1_{ns} = 2.133, while for mode 2, h^2_{fn} = 1.254, h^2_{ns} = 1.604 . Thus mode 2 unstabilizes at 1.604, value for which the linearization of mode 1 is a spiral focus.

Fig.8.2. Aperiodic intermittency for mode 1. Parameters as in Fig.8.1. Five trajectories with different pumping values are displayed.

Fig.8.3. Behavior of mode 1 for R=1.685. Parameters as in Fig.8.1. Note the resemblance with Silnikov's phenomenon.

Fig. 8.4. Heteroclinic phenomena at the origin: node attractor for weak mode. In the notations of eq. (2.12), $\gamma_1=1$, $\gamma_2= 2$, $\rho_1=1$, $\rho_2=0.7$, $\Delta_1= 0.8$, $\Delta_2= -0.5$, $S_1+2T_1= -0.5$, $S_2+2T_2 = 0.5$, $S_{12} = 2.5$, $T_{12}=0.125$. For mode 1 we get $h^1_{fn}= 0.8$, $h^1_{ns} = 1.2806$, while for mode 2, $h^2_{fn} = 0.35$, $h^2_{ns} = 2.95$. Thus mode 1 unstabilizes at 1.2806, value for which the linearization of mode 2 is a node attractor.

Fig.8.5. A possible cycle joining critical elements. For $n_2=0$, the trajectory stays a long time near $n_1=0$ and near $n_1=1,58$. Parameters as in Fig. 8.4, R = 1.30.

Fig.8.6. Linear dependence between the square of the frequency and the square of pumping power. Extrapolation to h=0 yields critical pumping = 1.274. From numerical simutations using the same parameters as in Fig.8.4.

Fig. 10.1. Symmetrical case: unperturbed phase portraits.

Fig. 10.2. Geometry of the Melnikov function.

Parallel pumping

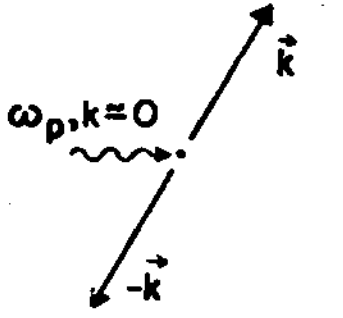

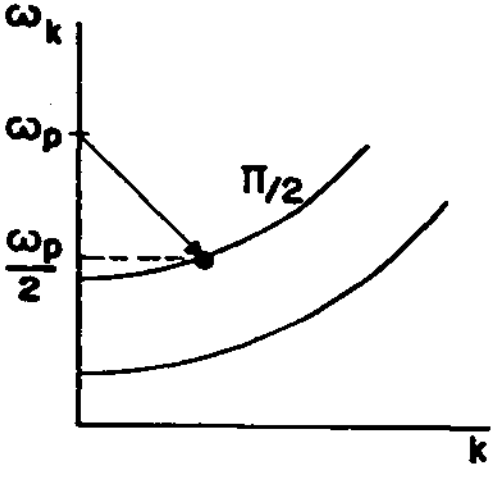

(a)

Perpendicular pumping

Subsiary Resonance

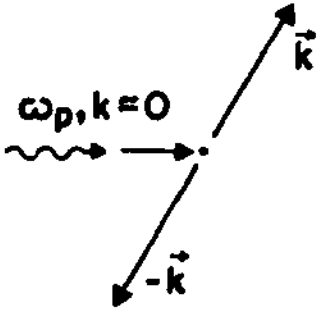

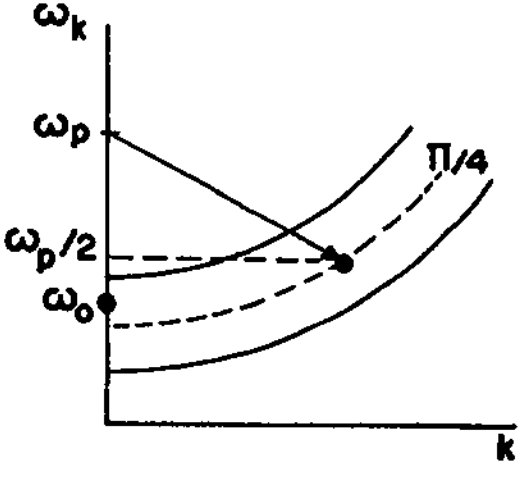

(b)

Fig.2.1

(a)

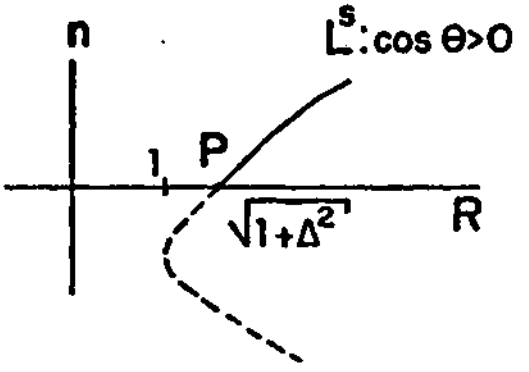

$n = \frac{1}{s}(-\Delta - \sqrt{R^2-1})$, $R \geqslant \sqrt{1+\Delta^2}$

$s<0 \quad \Delta<0$

(b)

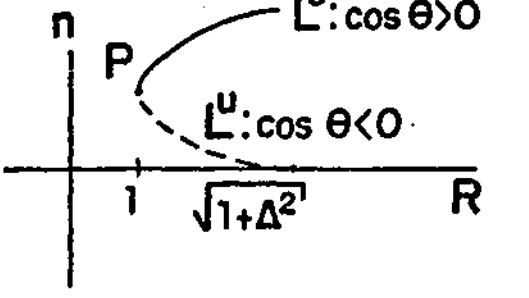

$n = \frac{1}{s}(-\Delta - \sqrt{R^2-1})$, $R \geqslant 1$

$s<0 \quad \Delta>0$

(c)

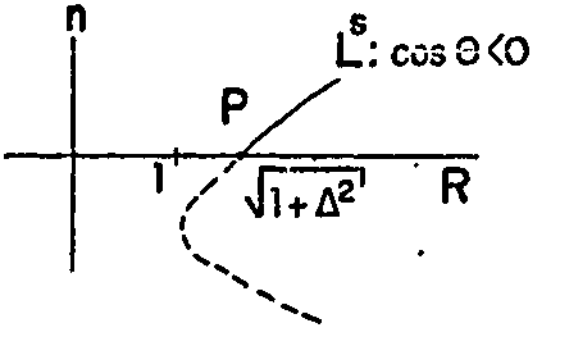

$n = \frac{1}{s}(-\Delta + \sqrt{R^2-1})$, $R \geqslant \sqrt{1+\Delta^2}$

$s>0 \quad \Delta>0$

(d)

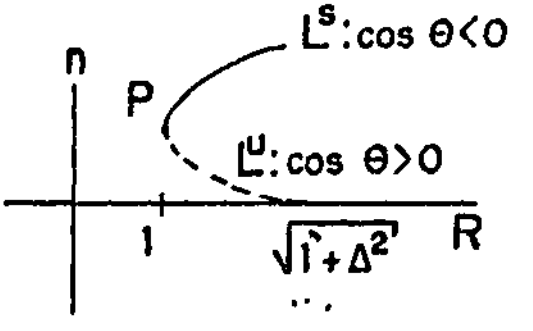

$n = \frac{1}{s}(-\Delta + \sqrt{R^2-1})$, $R \geqslant 1$

$s>0 \quad \Delta<0$

Fig.4.1

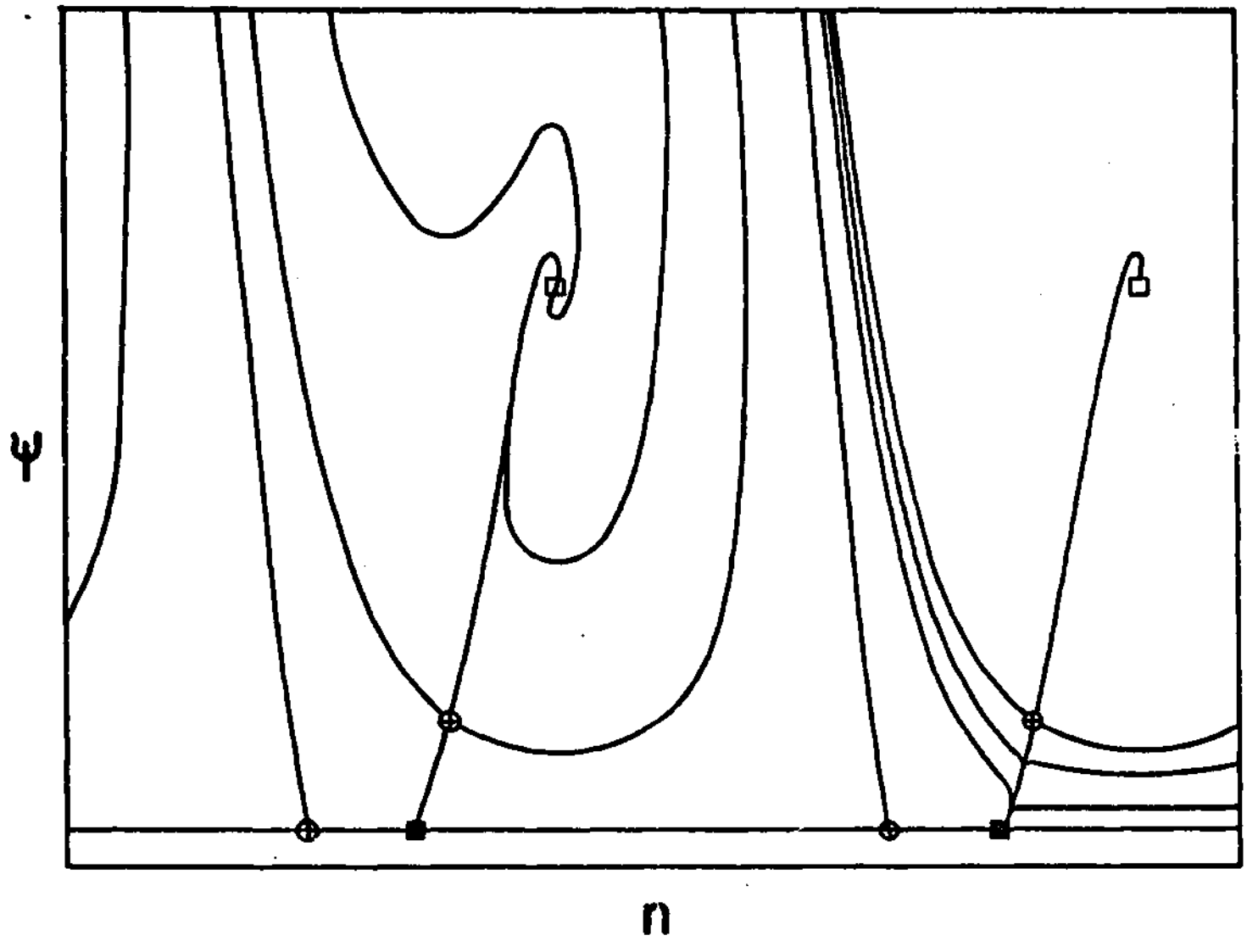

Fig.4.2

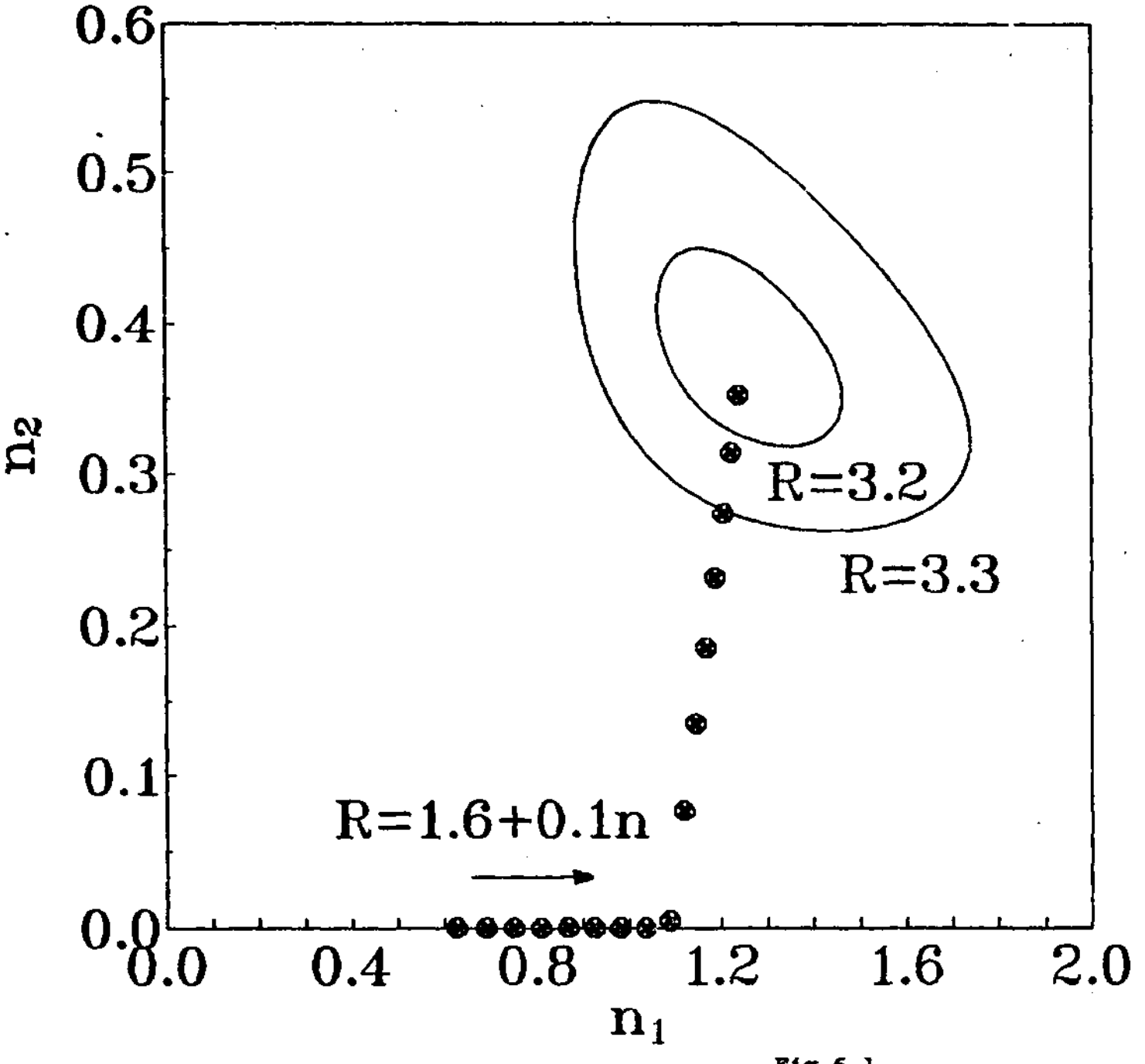

Fig.6.1

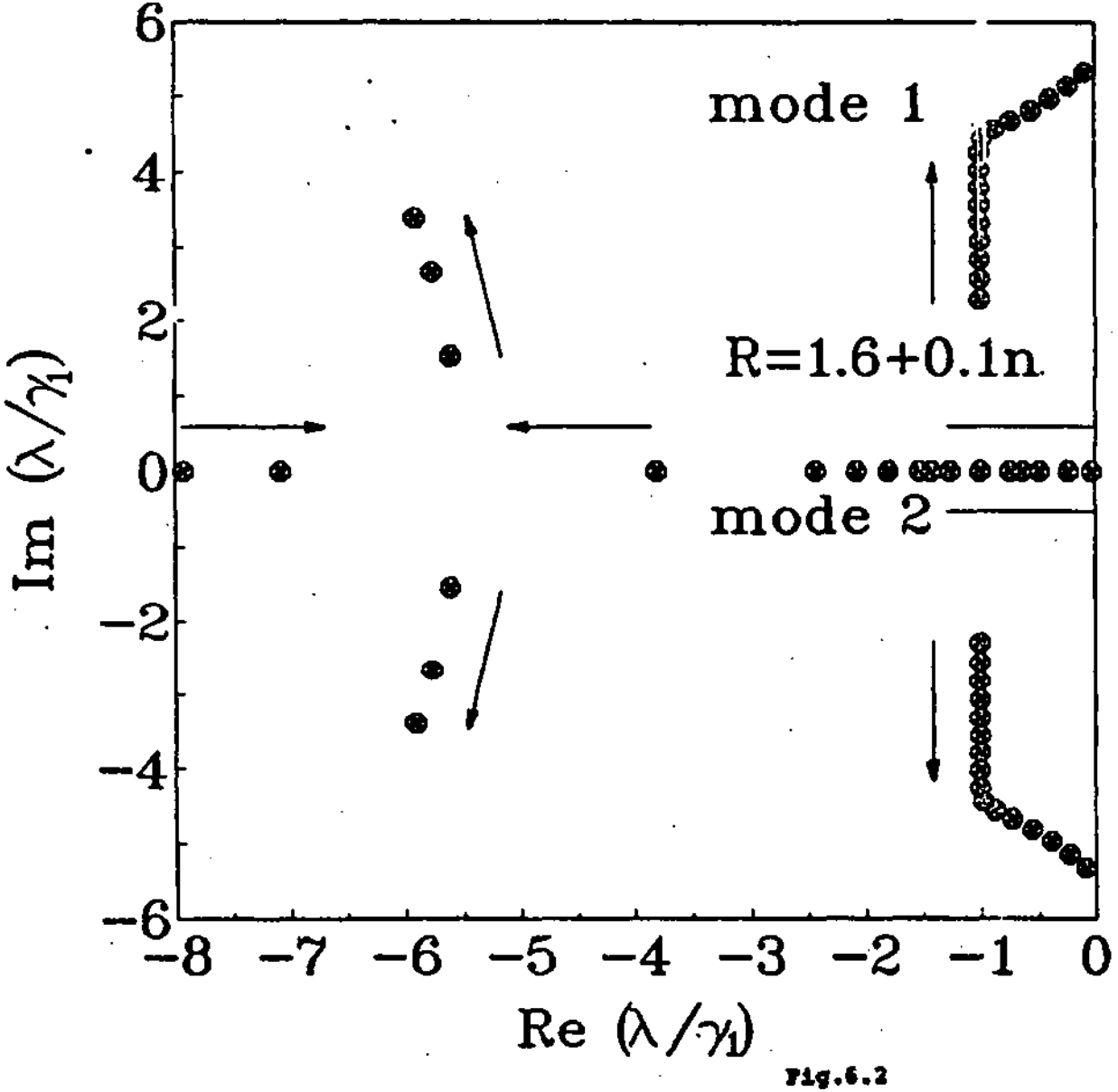

Fig.6.2

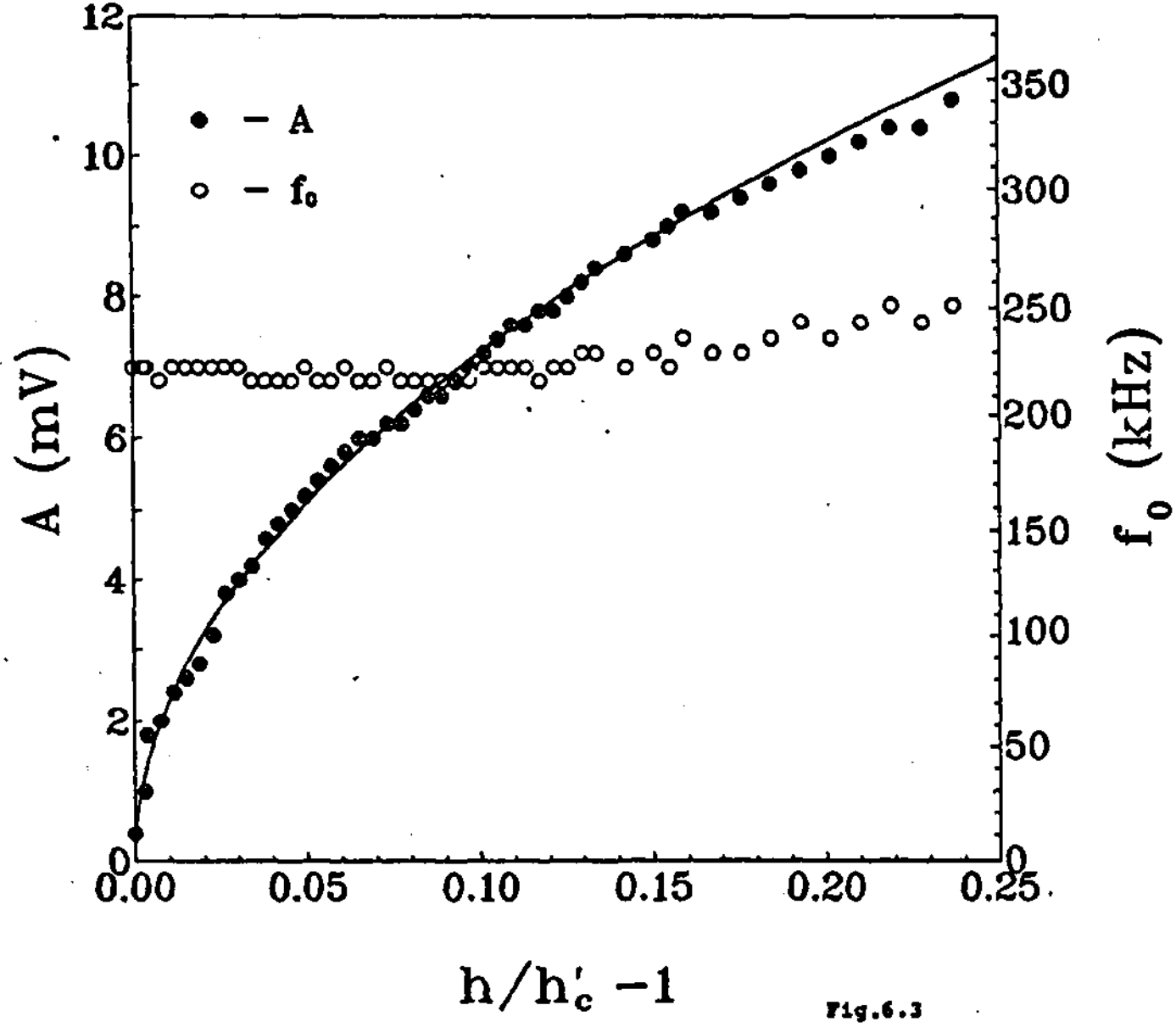
12
10
8
6
4
2
0
A (mV)
● – A
○ – f₀
350
300
250
200
150
100
50
0
f₀ (kHz)
0.00
0.05
0.10
0.15
0.20
0.25
h/h'c −1

Fig.6.3

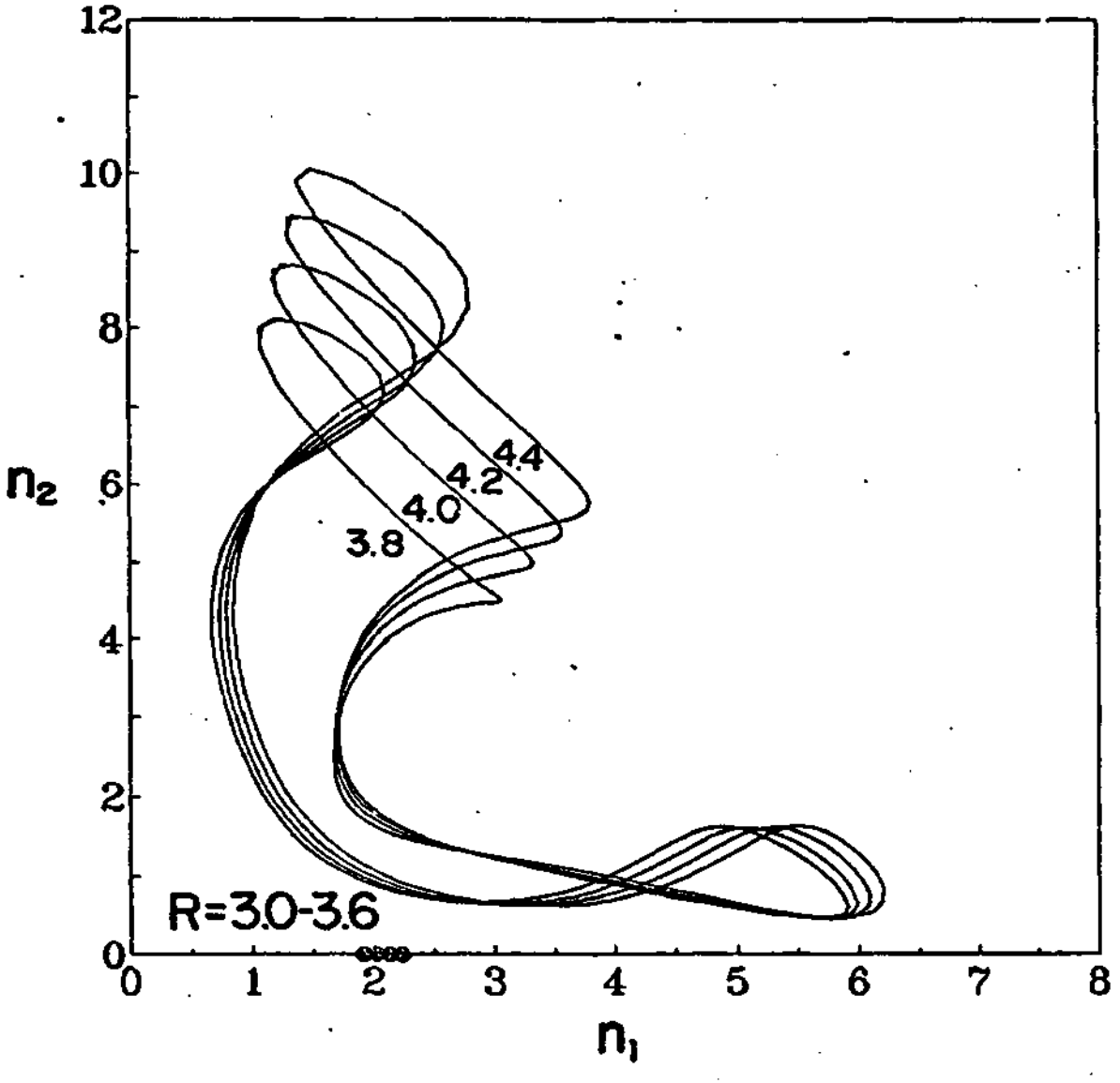

Fig.7.1

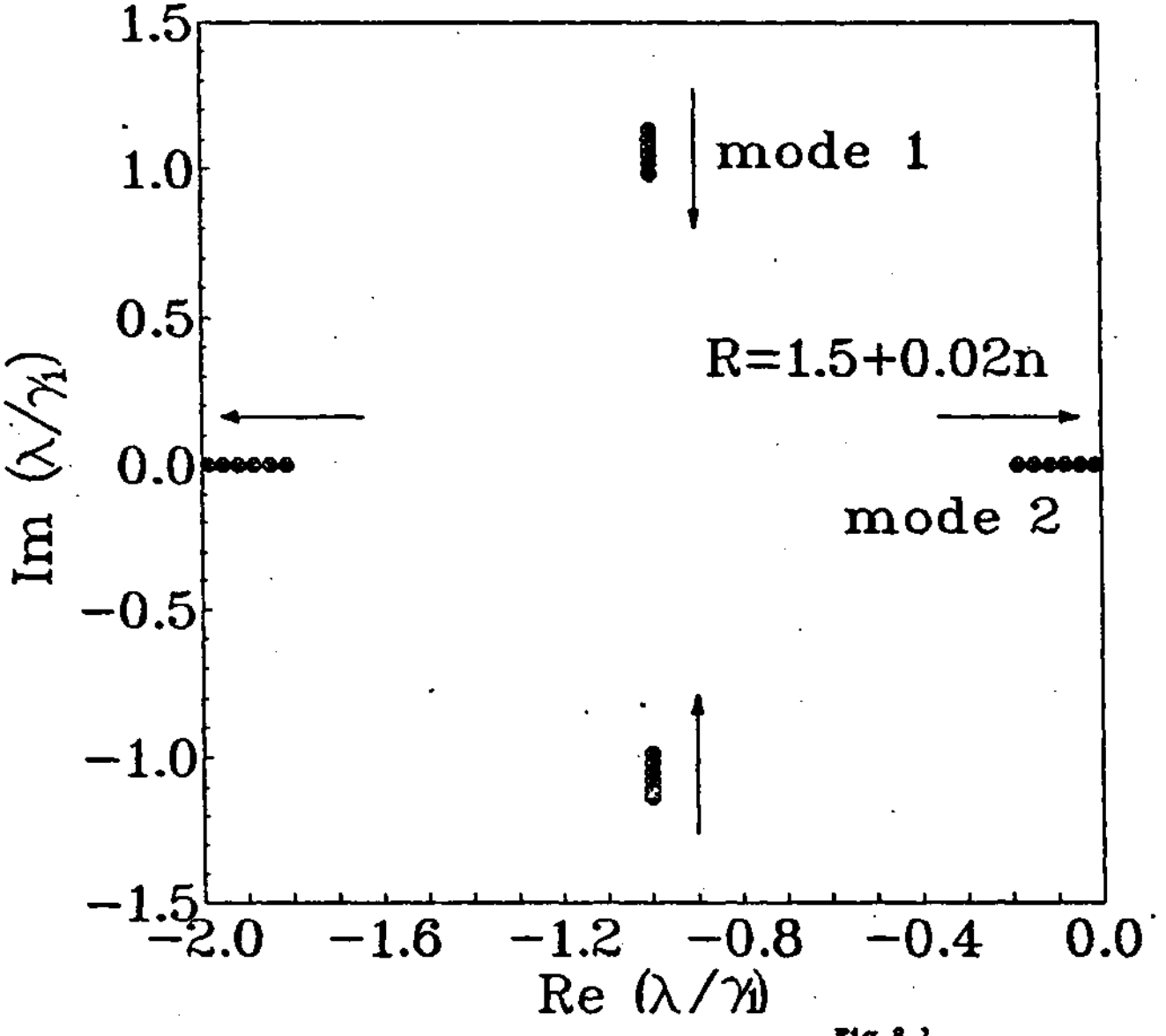
1.5
1.0
0.5
0.0
−0.5
−1.0
−1.5
−2.0
−1.6
−1.2
−0.8
−0.4
0.0
Im (λ/γ1)
Re (λ/γ1)
mode 1
mode 2
R=1.5+0.02n

Fig.8.1

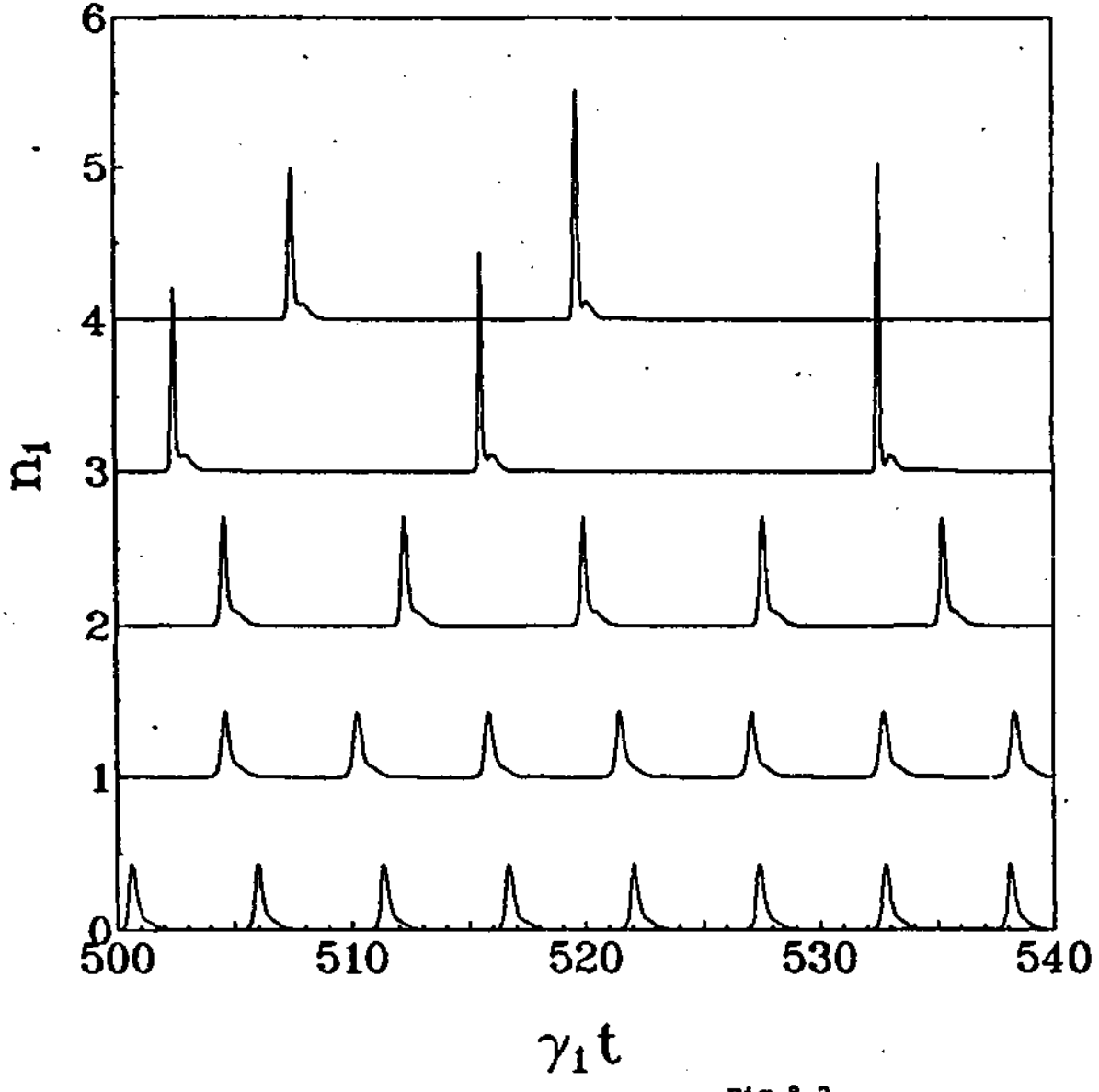

Fig.8.2

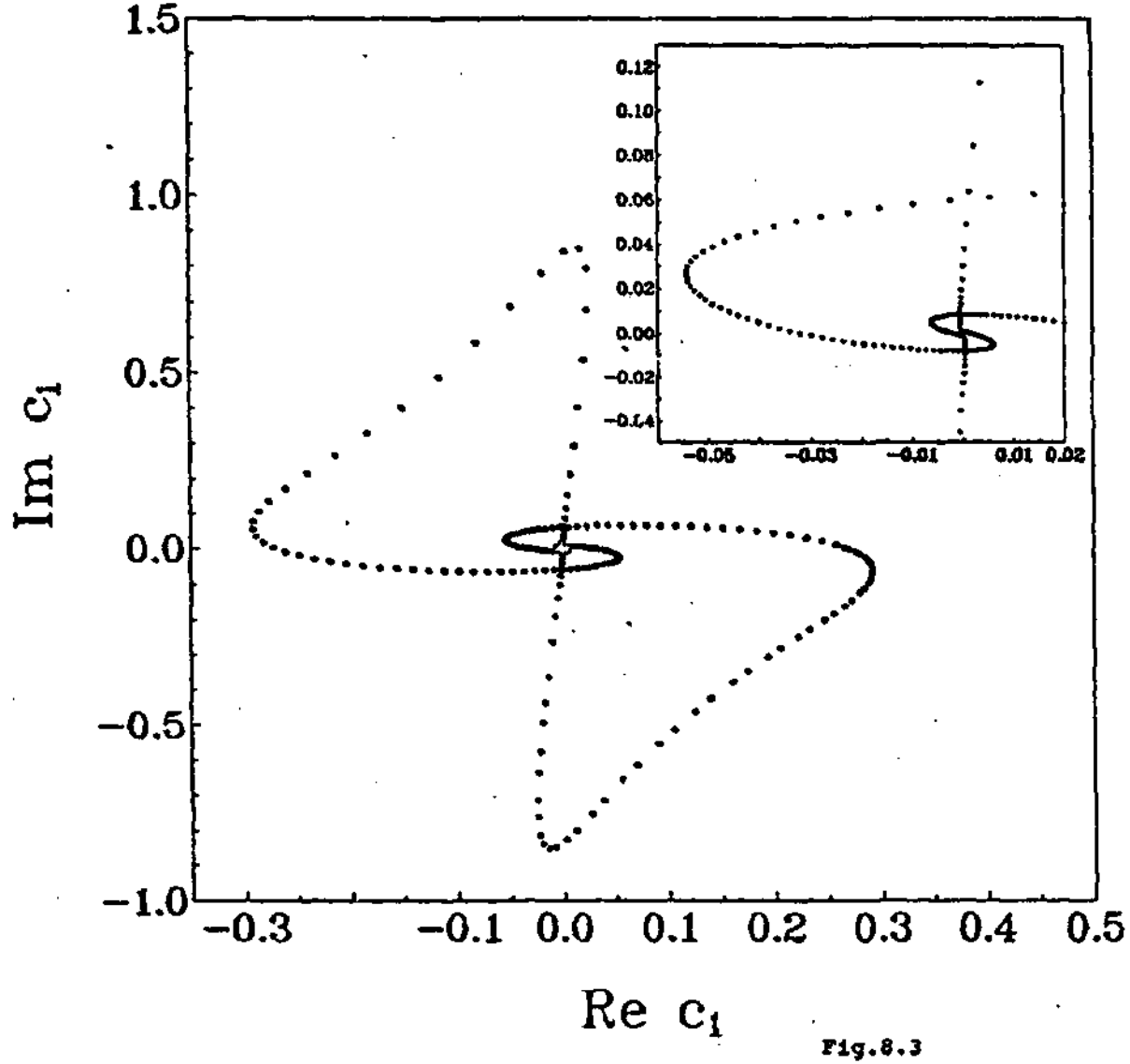
1.5
1.0
0.5
0.0
−0.5
−1.0
Im c_1
−0.3
−0.1
0.0
0.1
0.2
0.3
0.4
0.5
Re c_1
0.12
0.10
0.08
0.06
0.04
0.02
0.00
−0.02
−0.04
−0.05
−0.03
−0.01
0.01
0.02

Fig.8.3

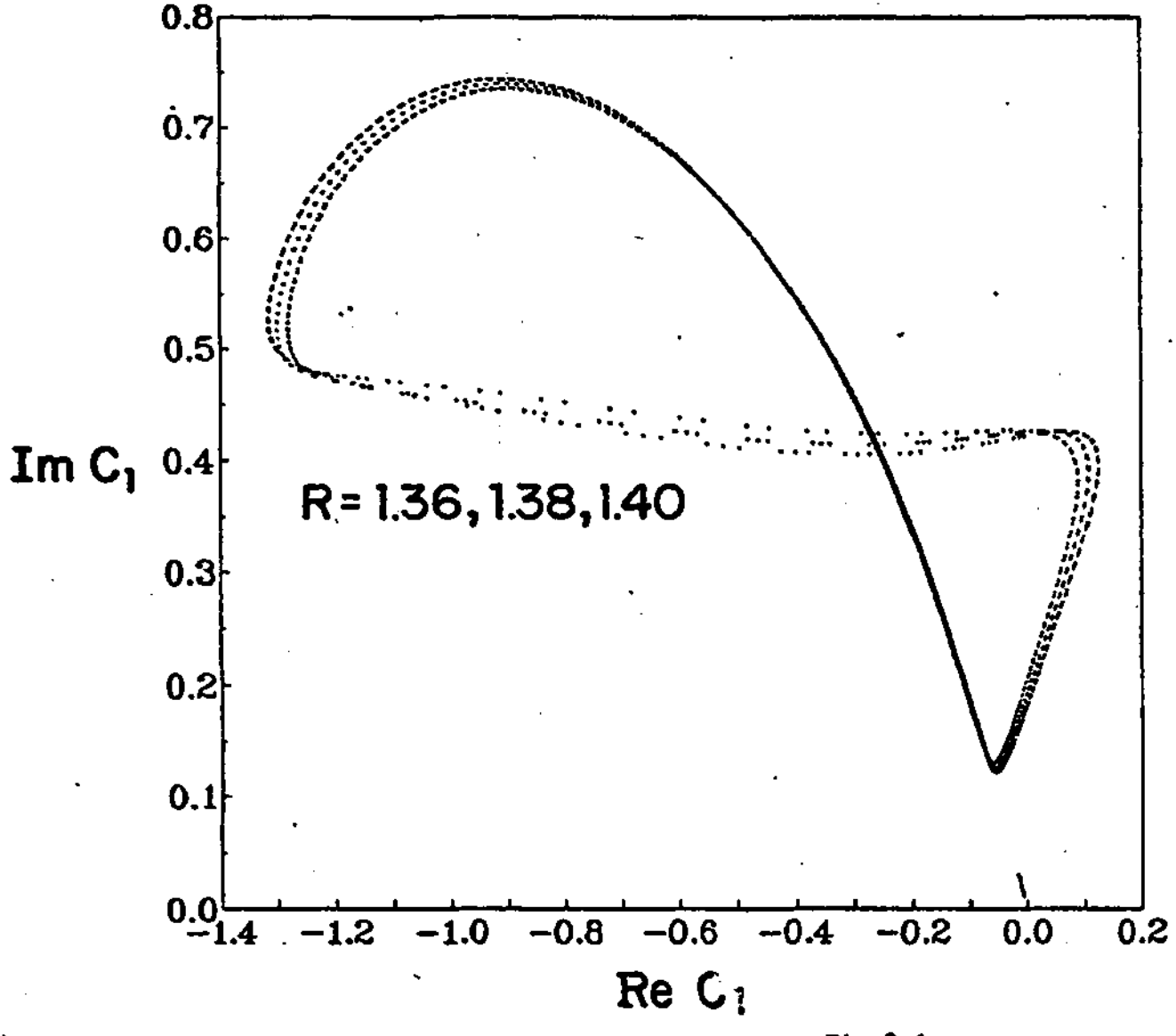
0.8
0.7
0.6
0.5
0.4
0.3
0.2
0.1
0.0
Im C1
R= 1.36, 1.38, 1.40
−1.4
−1.2
−1.0
−0.8
−0.6
−0.4
−0.2
0.0
0.2
Re C1

Fig.8.4

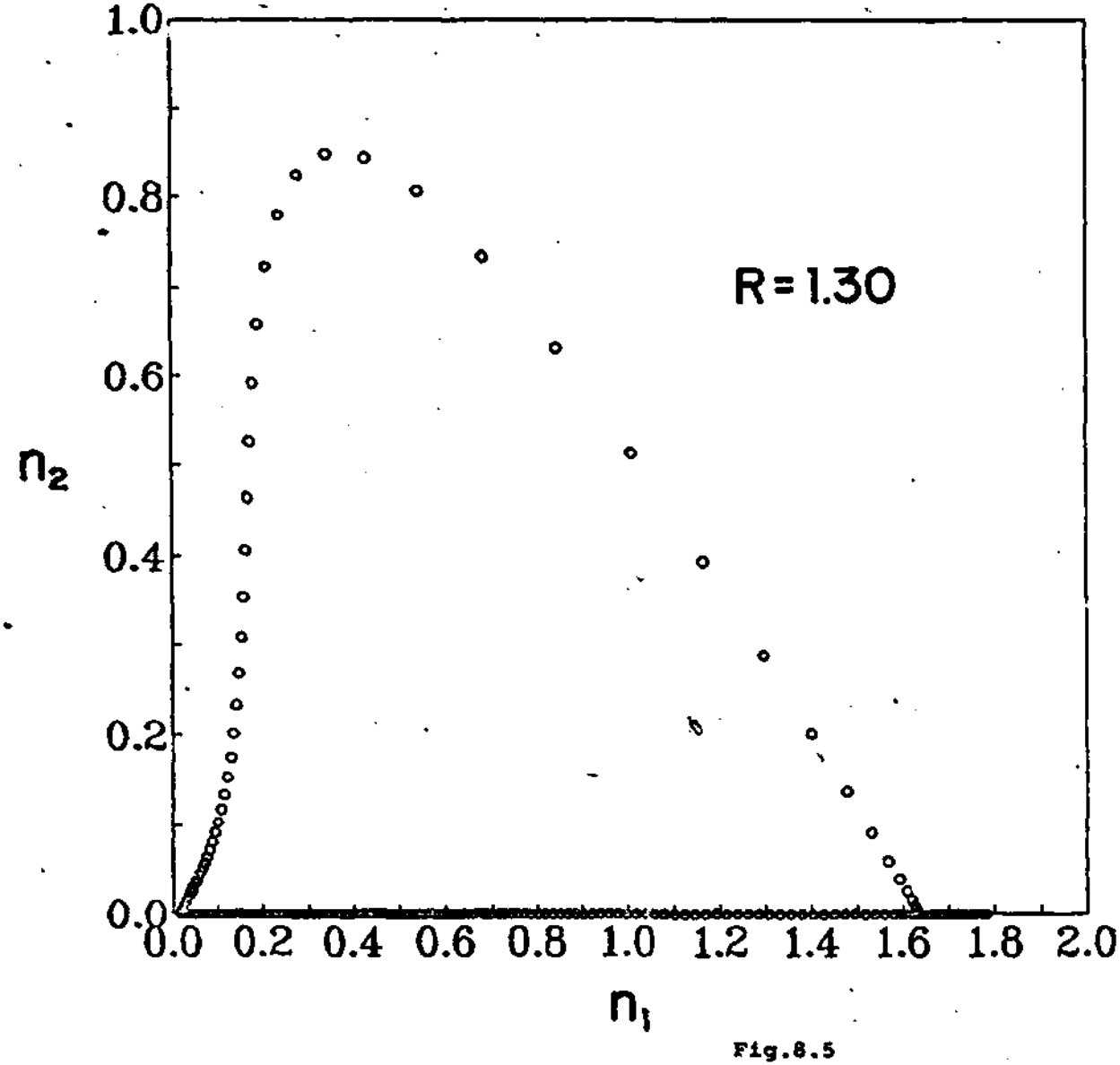

Fig.8.5

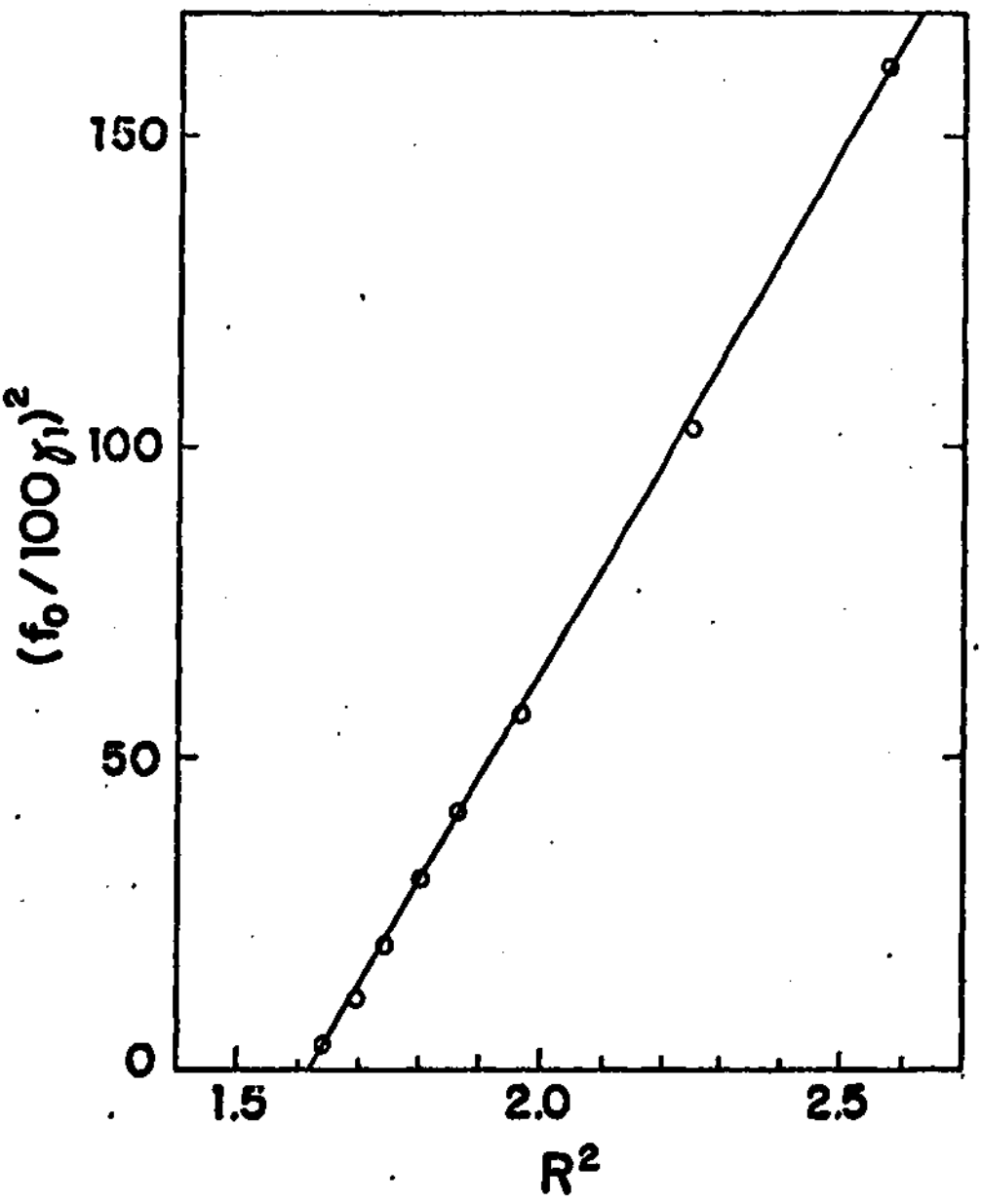

Fig.8.6

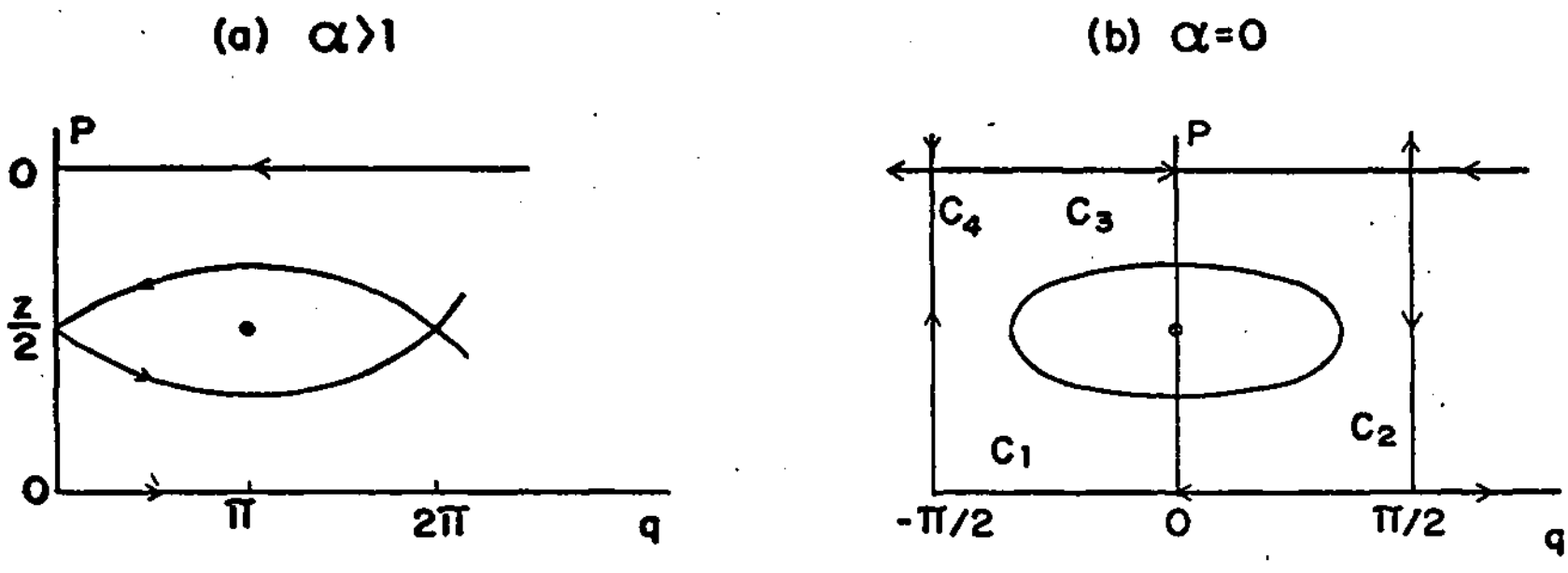

Fig.10.1

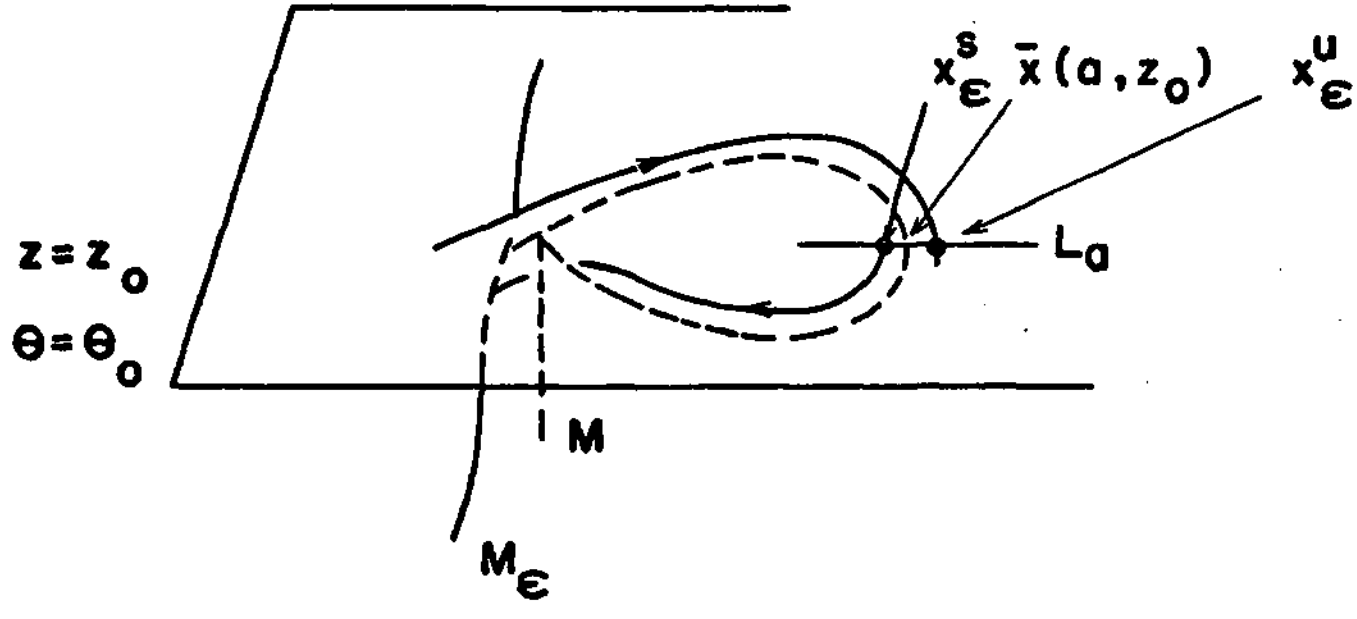
x^s_ϵ
$\bar{x}(a, z_0)$
x^u_ϵ
$z = z_0$
$\theta = \theta_0$
L_a
M
M_ϵ

Fig.10.2

ÚLTIMOS RELATÓRIOS DE PESQUISA E DESENVOLVIMENTO

LATEST RESEARCH AND DEVELOPMENT REPORTS

KUBRUSLY, C.S. *Strong stability does not imply similarity to a contraction.* 5 p. (RP&D 06/90)

FEIJÓO, R.A. & ZOUAIN, N. *Elastic-plastic potential functionals for rates and increments of stress and strain.* 23 p. (RP&D 07/90)

CARVALHO, R.L. *Abstract semantical systems.* 71 p. (RP&D 08/90)

MENEZES, C.S. & CARVALHO, R.L. *Processamento de conhecimento em ambientes multinivelados.* 65 p. (RP&D 09/90)

ZOUAIN, N.; FEIJÓO, R.A. & HECKE, M. *A contribution to structural plasticity by optimization techniques - Part II. Analysis of model discretization and mathematical programming algorithms for elastic-plastic incremental analysis.* 20 p. (RP&D 10/90)

PEREIRA, D.C. & MENZALA, G.P. *Exponential stability in linear thermoelasticity: the inhomogeneous case.* 17 p. (RP&D 11/90)

LUCENA, ABÍLIO *The cost convergence algorithm for the Bottleneck transportation problem.* 11 p. (RP&D 12/90)

CORREA, G.O. *On bounded-input/bounded-state stability for discrete-time, bilinear systems.* 39 p. (RP&D 13/90)

FERREIRA, JORGE & PEREIRA, D.C. *On a nonlinear degenerate evolution equation with strong damping.* 12 p. (RP&D 14/90)

RIVERA, JAIME. *Pointwise control: Differentiability of the optimal cost function.* 7 p. (RP&D 15/90)

LONDRES, HELENA *O uso da algebra booleana em analises qualitativas e comparativas.* 32 p. (RP&D 16/90)

COSTA, M.L.; SAMPAIO, R. & DA GAMA, R.M.S. *Local description of the energy transfer process in a packed bed heat exchanger.* 19 p. (RP&D 17/90)

KARAM, JOSÉ & LOULA, ABIMAEL. *A non-standard application of Babuška-Brezzi theory to finite element analysis of stokes problem.* 26 p. (RP&D 18/90)

FRANCA, L.P.; KARAM, J.; LOULA, ABIMAEL & STENBERG, R. *A convergence analysis of a stabilized method for the Stokes flow.* 7 p. (RP&D 19/90)

BORDONI, PAULO. *Approximating the nonlinear Schrödinger equation in $\mathbb{R}^2$ by the nonlinear Schrödinger equation in open bounded convex sets.* 14 p. (RP&D 20/90)

FANCELLO, E.; SALGADO, A.C. & FEIJÓO, R.A. *Aranha: gerador de malhas 2D para elementos finitos triangulares de 3 e 6 nós.* 13 p. (RP&D 21/90)

KUBRUSLY, L.S. *Uma estratégia de análise multivariada.* 18 p. (RP&D 22/90)

SALDANHA DA GAMA, R.M. *On the physical solutions to the heat equation subjected to nonlinear boundary conditions.* 12 p. (RP&D 23/90)

FRAGOSO, M.D. & DE SOUZA, C.E. *On the existence of maximal solution for generalized algebraic Riccati equations arising in stochastic control.* 16 p. (RP&D 24/90)

HEMERLY, E.M. & FRAGOSO, M.D. *Will the PLS criterion for order estimation work with AML and a posteriori prediction error?* 16 p. (RP&D 25/90)

SALDANHA DA GAMA, R.M. *Dynamical analysis of a compressible elastic rod in the current configuration.* 17 p. (RP&D 26/90)
RIVERA, J.E.M. *Energy decay rates in linear thermoelasticity.* 14 p. (RP&D 27/90)
MURAD, M.A. & LOULA, ABIMAEL. *Improved accuracy in finite element analysis of Biot's consolidation problem.* 31 p. (RP&D 28/90)
RIVERA, J.M. *Decomposition of the displacement vector field and decay rates in linear thermoelasticity.* 28 p. (RP&D 29/90)
CORREA, HELIO & HUGHES, THOMAS. *The finite element method with Lagrange multipliers on the boundary: circumventing the Babuška-Brezzi condition.* 27 p. (RP&D 30/90)
KUBRUSLY, R.S. *A direct dual method for nonlinear eigenvalue inequalities.* 7 p. (RP&D 31/90)
FRANCA, L.P.; FREY, SERGIO & HUGHES, THOMAS. *Stabilized finite element methods: I. application to the advective-diffusive model.* 45 p. (RP&D 32/90)
SILVEIRA, M.A. & CORRÊA, G.O. *On H_2 optimal control of linear systems under tracking/disturbance rejection constraints.* 40 p. (RP&D 33/90)
ZOUAIN, N.; BORGES, L.; HERSKOVITS, J. & FEIJÓO, R. *An iterative algorithm for limit analysis with nonlinear yield functions.* 26 p. (RP&D 34/90)
FANCELLO, E.; FEIJÓO, R. & ZOUAIN, N. *Formulação variacional do problema de contato com atrito; resolução via regularização.* 16 p. (RP&D 35/90)
ZOUAIN, N.; FEIJÓO, R.; HECKE, M. & BEVILACQUA, L. *Potential constitutive relations for plasticity using internal variables.* 16 p. (RP&D 36/90)
LOIS ANIDO, J.C.; HERSKOVITS, J.; FEIJÓO, R. & TAROCO, E.O. *Otimização da forma de corpos elásticos planos para redução de concentração de tensões.* 11 p. (RP&D 37/90)
HUESPE, A.; LOPES, J.L.; BORGES, L.; ZOUAIN, N. & FEIJÓO, R. *Elementos mistos triangulares para análise limite: Part I. Formulação.* 10 p. (RP&D 38/90)
BORGES, L.; LOPES, J.L.; HUESPE, A.; ZOUAIN, N.; FEIJÓO, R. & HERSKOVITS, J. *Elementos mistos triangulares para análise limite: Part II. Resolução iterativa e aplicações.* 10 p. (RP&D 39/90)
CORRÊA, G.O. & SILVEIRA, M.A. *On the parametrization of all solutions to a servomechanism problem.* 20 p. (RP&D 40/90)

Pedidos de cópias devem ser enviados ao:
Request for free copies should be addressed to:

Laboratório Nacional de Computação Científica
Rua Lauro Müller 455
22290, Rio de Janeiro, R.J.
Brasil

Impressão&Produção
Gráfica do LNCC

Secretaria Especial da Ciência e Tecnologia
Conselho Nacional de Desenvolvimento Científico e Tecnológico

Laboratório Nacional de Computação Científica

Rua Lauro Muller, 455 - Caixa Postal 56018 - 22290 - Rio de Janeiro - RJ - Brasil